



HAL
open science

Tree species growth response to climate in mixtures of *Quercus robur*/*Quercus petraea* and *Pinus sylvestris* across Europe - a dynamic, sensitive equilibrium

Sonja Vospernik, Michael Heym, Hans Pretzsch, Maciej Pach, Mathias Steckel, Jorge Aldea, Gediminas Brazaitis, Andrés Bravo-Oviedo, Miren del Rio, Magnus Löff, et al.

► To cite this version:

Sonja Vospernik, Michael Heym, Hans Pretzsch, Maciej Pach, Mathias Steckel, et al.. Tree species growth response to climate in mixtures of *Quercus robur*/*Quercus petraea* and *Pinus sylvestris* across Europe - a dynamic, sensitive equilibrium. *Forest Ecology and Management*, 2023, 530, pp.120753. 10.1016/j.foreco.2022.120753 . hal-04211027

HAL Id: hal-04211027

<https://hal.inrae.fr/hal-04211027>

Submitted on 19 Sep 2023

HAL is a multi-disciplinary open access archive for the deposit and dissemination of scientific research documents, whether they are published or not. The documents may come from teaching and research institutions in France or abroad, or from public or private research centers.

L'archive ouverte pluridisciplinaire **HAL**, est destinée au dépôt et à la diffusion de documents scientifiques de niveau recherche, publiés ou non, émanant des établissements d'enseignement et de recherche français ou étrangers, des laboratoires publics ou privés.



Distributed under a Creative Commons Attribution 4.0 International License

1 **Tree species growth response to climate in mixtures of *Quercus robur*/*Quercus petraea***
2 **and *Pinus sylvestris* across Europe - a dynamic, sensitive equilibrium**

3 Sonja Vospernik^{a*}, Michael Heym^b, Hans Pretzsch^c, Maciej Pach^d, Mathias Steckel^e, Jorge Aldea^f, Gediminas
4 Brazaitis^g, Andrés Bravo-Oviedo^h, Miren Del Rioⁱ, Magnus Löf^f, Marta Pardosⁱ, Kamil Bielak^j, Felipe Bravo^k,
5 Lluís Coll^{l,m}, Jakub Černýⁿ, Lars Droessler^o, Martin Ehbrecht^p, Aris Jansons^q, Nathalie Korboulewsky^f, Marion
6 Jourdan^s, Thomas Nord-Larsen^t, Arne Nothdurft^a, Ricardo Ruiz-Peinadoⁱ, Quentin Ponette^u, Roman Sitko^v,
7 Miroslav Svoboda^w, Barbara Wolff^x

8 a Department of Forest- and Soil Sciences, Institute of Forest Growth, BOKU, University of Natural
9 Resources and Life Sciences Vienna, Peter-Jordan-Str. 82, A-1190 Vienna. Austria

10 b Bavarian State Institute of Forestry (LWF), Department Silviculture and Mountain Forest, Germany

11 c Chair of Forest Growth and Yield Science, Department of Life Science Systems, TUM School of
12 Life Sciences, Technical University of Munich. Hans-Carl-Von-Carlowitz-Platz 2, 85354 Freising,
13 Germany

14 d Department of Ecology and Silviculture, Faculty of Forestry, University of Agriculture in Krakow,
15 al. 29-Listopada 46 31-425 Kraków, Poland

16 e Forst Baden-Württemberg (AöR), Forstbezirk Ulmer Alb, Schloßstr. 34. 89079 Ulm-Wiblingen.
17 Germany

18 f Swedish University of Agricultural Sciences, Southern Swedish Forest Research Centre, Box 190.
19 23422 Lomma, Sweden

20 g Vytautas Magnus University, Department of Forest Science, Studentu 11, Akademija LT-53361.
21 Kaunas dist, Lithuania

22 h Dpt. Biogeography and Global Change, National Museum of Natural Sciences – CSIC. Serrano 115.
23 28006 Madrid. Spain

24 i Instituto de Ciencias Forestales ICIFOR, INIA-CSIC, Ctra. A Coruña km 7.5. 28040 Madrid, Spain

25 j Department of Silviculture, Institute of Forest Sciences, Warsaw University of Life Sciences,
26 Nowoursynowska 159/34, 02776 Warsaw, Poland

27 k Department of Plant Production and Forest Resources, Higher Technical School of Agricultural
28 Engineering of Palencia, University of Valladolid, Spain

29 l Department of Agriculture and Forest Engineering (EAGROF), University of Lleida, Lleida, Spain

30 m Joint Research Unit CTFC-AGROTECNIO-CERCA, Solsona, Spain

31 n Forestry and Game Management Research Institute, Strnady 136, 252 02 Jíloviště, Czech Republic

32 o School of Natural Sciences and Medicine, Ilia State, University, Kakutsa Cholokashvili Ave 3/5.
33 0162 Tbilisi, Georgia

34 p Silviculture and Forest Ecology of the Temperate Zones and Centre for Biodiversity and Sustainable
35 Landuse, University of Göttingen, Büsgenweg 1, Göttingen, German

36 q Latvian State Forest Research Institute Silava, Rigas 111, Salaspils. Latvia

37 r French National Institute for Agriculture, Food. and Environment (INRAE), UR EFNO - Centre de
38 recherche Val de Loire, 45290 Nogent-Sur-Vernisson, France

39 s Université de Lorraine, AgroParisTech, INRAE, UMR Silva, 54000, Nancy, France

40 t Department of Geosciences and Natural Resource Management, University of Copenhagen,
41 Rolighedsvej 23, Frederiksberg C, Denmark

42 u UCLouvain - Université catholique de Louvain, Earth & Life Institute, Croix du Sud 2 box
43 L7.05.09. 1348 Louvain-la-Neuve. Belgium

44 v Technical University in Zvolen, Faculty of Forestry, Department of Forest Resource Planning and
45 Informatics, T. G. Masaryka 24, 96001 Zvolen, Slovakia

46 w Faculty of Forestry and Wood Sciences, Czech University of Life Sciences, Prague, Czech Republic

47 x Hochschule für nachhaltige Entwicklung Eberswalde (HNEE), FG Waldinventur und Planung,
48 Alfred-Möller-Str.1, D 16225 Eberswalde, Germany

49

50 *Corresponding author. Sonja Vospernik. University of Natural Resources and Life Sciences. Vienna.
51 Department of Forest and Soil Sciences. Institute of Forest Growth. Peter-Jordan-Str. 82. A-1190
52 Vienna. Austria

53 E-mail address: Sonja.Vospernik@boku.ac.at

54 Phone: ++43-1-47654/91412

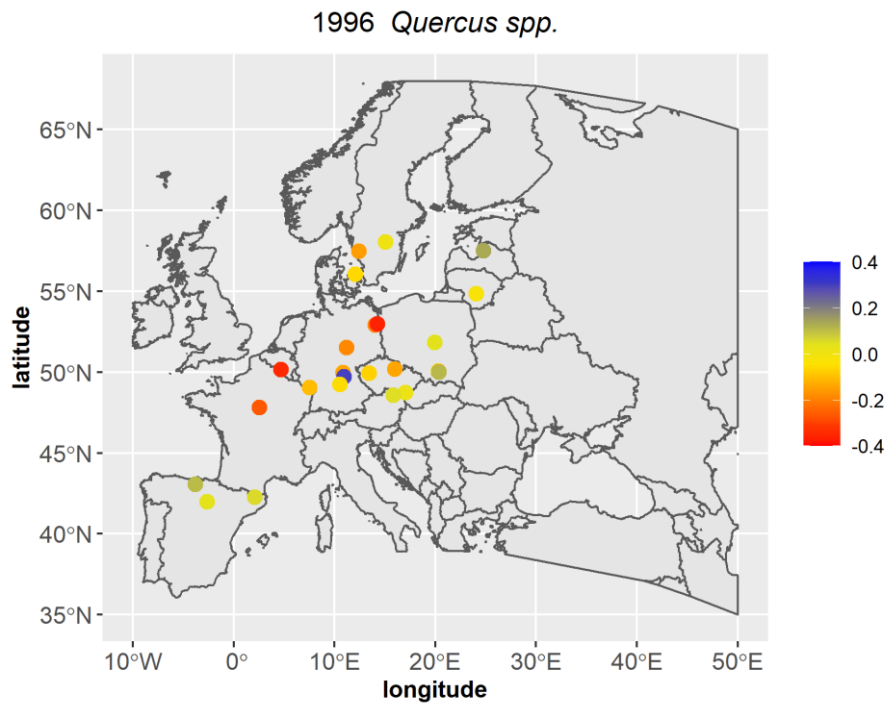
55

56 **Abstract**

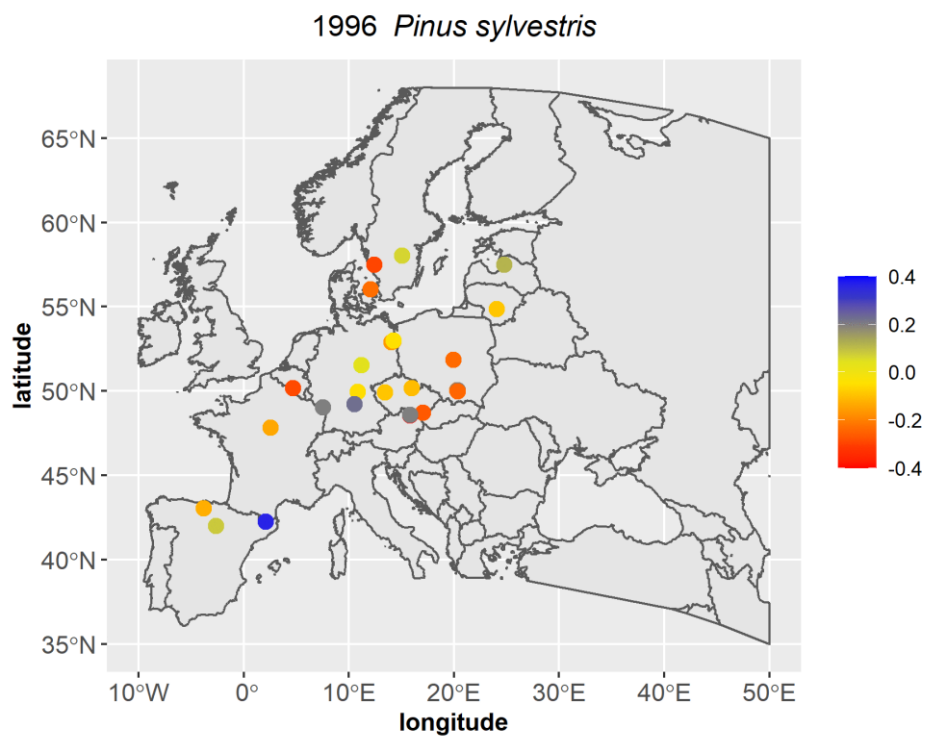
57 *Quercus robur/Quercus petraea* and *Pinus sylvestris* are widely distributed and economically
58 important tree species in Europe co-occurring on mesotrophic, xeric and mesic sites.
59 Increasing dry conditions may reduce their growth, but growth reductions may be modified by
60 mixture, competition and site conditions. The annual diameter growth in monospecific and
61 mixed stands along an ecological gradient with mean annual temperatures ranging from 5.5°C
62 to 11.5°C was investigated in this study. On 36 triplets (108 plots), trees were cored and the
63 year-ring series were cross-dated, resulting in year-ring series of 785 and 804 trees for *Q. spp.*
64 and *P. sylvestris*, respectively. A generalized additive model with a logarithmic link was fit to
65 the data with random effects for the intercept at the triplet, year and tree level and a random
66 slope for the covariate age for each tree; the Tweedie-distribution was used. The final model
67 explained 87 % of the total variation in diameter increment for both tree species. Significant
68 covariates were age, climate variables (long-term mean, monthly), local competition
69 variables, relative dbh, mixture, stand structure and interactions thereof. Tree growth declined
70 with age and local density and increased with social position. It was positively influenced by
71 mixture and structural diversity (Gini coefficient); mixture effects were significant for *P.*
72 *sylvestris* only. The influence of potential evapotranspiration (PET) in spring and autumn on
73 tree growth was positive and non-linear, whereas tree growth sharply decreased with
74 increasing PET in June, which proved to be the most influential month on tree growth along
75 the whole ecological gradient. Interactions of PET with tree social position (relative dbh)
76 were significant in July and September for *Q. spp.* and in April for *P. sylvestris*. Interactions
77 of climate with density or mixture were not significant. Climatic effects found agree well with
78 previous results from intra-annual growth studies and indicate that the model captures the
79 causal factors for tree growth well. Furthermore, the interaction between climate and relative
80 dbh might indicate a longer growth duration for trees of higher social classes. Analysis of

81 random effects across time and space showed highly dynamic patterns, with competitive
82 advantages changing annually between species and spatial patterns showing no large-scale
83 trends but pointing to the prevalence of local site factors. In mixed-species stands, the tree
84 species have the same competitiveness in the long-term, which is modified by climate each year.
85 Climate warming will shift the competitive advantages, but the direction will be highly site-
86 specific.

87 Graphical abstract



88



89

90 A random intercept for each triplet and year for *Quercus robur* and *Quercus petraea* (top) and *Pinus sylvestris*
91 (bottom) showing the inter-annual variation in diameter increment on different sites at the logarithmic scale in
92 mm

1. Introduction

Quercus robur/Quercus petraea (*Q. spp.* hereafter) and *Pinus sylvestris* are economically important tree species constituting a considerable proportion of the forest cover in Europe (Eaton et al. 2016, Durrant et al. 2016). All three species range from southern Europe (Iberian peninsula, Greece) to Scandinavia, but *P. sylvestris* grows on a wider latitudinal and longitudinal range (Eaton et al. 2016, Durrant et al. 2016) than *Q. spp.*. The two *Quercus* species naturally hybridize, forming fertile offspring, so that they are viewed as sub-species by some authors (e.g. Roloff und Bärtels 2006). Because of their considerable range overlap, frequent hybridization and similar ecology, the two species are often investigated jointly.

Q. spp. and *P. sylvestris* are light-demanding tree species growing in a mixture on xeric and mesic, acidophilous sites where they represent the climatic climax (Muller 1992, Eaton et al. 2016, Durrant et al. 2016). The exigency for nutrients is lower for *P. sylvestris* than for *Q. spp.* (Mellert et al. 2012). *Q. spp.* are thermophilic, and they grow on sites with a minimum of 8.4°C during the growing season, while the temperature range of the pioneer species *P. sylvestris* is considerably larger (Vospornik 2021). All three tree species have been recognized as drought tolerant and with an efficient protection against high irradiance (*Q. spp.*: Epron and Dreyer 1993, Arend et al. 2011, Bose et al. 2021, Vitasse et al. 2019, *P. sylvestris*: Eilmann et al. 2006, Rigling et al. 2001). *Q. spp.* have deep penetrating tap roots and are an-isohydric tree species, known to keep their stomata open under drought conditions, showing a good resistance and resilience to drought and consequently a small decrease in tree growth in drought years (Trouvé et al. 2017, Leuzinger et al. 2005). Comparative studies on *Q. robur* and *Q. petraea*. reported only slight differences between the two species, with *Q. petraea* being more drought tolerant because of its higher intrinsic water-use efficiency (Epron and Dreyer 1993, Arend et al. 2011).

119 *P. sylvestris* is also well adapted to a dry climate, but as conifer species, has a more
120 conservative water use strategy. It can be classified as an iso-hydric species, closing its
121 stomata earlier under drought conditions (Martín-Gómez et al. 2017, Zweifel 2009), which
122 leads to carbon starvation and a long-term reduction of the needle mass (Rigling et al. 2001,
123 Zweifel 2009). Subsequently, carbon starvation is thought to result in mortality, and higher
124 mortality rates under drought were observed for *P. sylvestris* than for both *Q. spp.* (Bigler et
125 al. 2006, Eilmann et al. 2006). In the last years, *P. sylvestris* has suffered tremendously from
126 heat waves (Salomon et al. 2022), which may result in a species shift in favor of *Q. spp.* on
127 dry sites with increasing climate warming (Eilmann et al. 2006).

128 While tree growth in the South of Europe is limited by summer drought, imposed by
129 the Mediterranean climate, tree growth in Central regions, exhibiting mesic growing
130 conditions, is more dependent on the competitive potential (Ramírez-Valiente et al. 2020). In
131 the Mediterranean climate, however, both *P. sylvestris* and *Q. spp.* show unimodal growth
132 patterns. Tree growth starts in spring, showing a maximum around the summer solstice and a
133 decline in late summer and autumn with the growing season being shorter on the more
134 drought prone sites (Strieder and Vospernik 2021). As a consequence of this tree growth
135 pattern, drought effects vary with season (Merlin et al. 2015), and spring or early summer
136 droughts have a more substantial impact on tree growth (Bose et al. 2021). *P. sylvestris* is an
137 evergreen conifer, which starts to grow when the temperature rises above 5 °C. As ring-
138 porous trees, *Q. spp.* do not come into leaf until late April-May (Eaton et al. 2016), although
139 their growth starts before budburst (Suzuki et al. 1996).

140 Tree ring analysis is an important and frequently used way to investigate climate-
141 growth relationships (Linderholm 2001, Mérian et al. 2013). Since the tree species studied
142 here are widespread, many tree ring studies have been carried out to analyse their growth (e.g.
143 Barsoum et al. 2015, Trouvé et al. 2017). Previous studies reported that *Q. spp.* and *P.*
144 *sylvestris* respond to drought with reduced ring width, but fluctuations in ring width are less

145 pronounced for *Q. spp.* because of its an-isohydric nature (Zweifel 2009) and tree growth at
146 high elevations was reported to show less between year variation (Vospernik and Nothdurft
147 2018) than tree growth at lower ones; Similarly, a response to long-term drought was reported
148 for higher elevations, whereas a response to short-term drought was observed at lower
149 elevation sites (Bhuyan et al. 2017). These previous studies, however, focus on a specific area
150 and do not encompass the whole climatic gradient where both *Q. spp.* and *P. sylvestris* co-
151 occur, nor do they explicitly include mixture or competition effects, which may be prevalent
152 in a temperate climate.

153 Growth related mixture effects for *Q. spp./P. sylvestris*, which occupy a similar
154 ecological niche, are reported to be positive on average, with a range between 6-14 % and
155 considerable variation between sites (Steckel et al. 2019, Steckel et al. 2020a, Pretzsch et al.
156 2020). The competitive advantage for *P. sylvestris* in the mixture increases with site index and
157 water supply, while it decreases with site index for *Q. spp.* (Pretzsch et al. 2020). Differences
158 in productivity between monospecific and mixed stands at the stand level may result from
159 higher stand densities, higher inequality of tree size distribution and growth-size relationships
160 with stronger size asymmetry and emergent properties derived from effects at the tree level
161 (Pretzsch and Schütze 2016). In contrast, at the individual tree level possible reasons for
162 positive mixture effects are tree specific differences in the crown and root morphology, water
163 and nutrient use strategy, different leaf and litter composition and tree phenology (Kelty et al.
164 1992, Pretzsch and Schütze 2016, Ammer 2019). At the individual tree level *Q. spp.* profited
165 on average from the admixture of *P. sylvestris* (Toïgo et al. 2018) or behaved indifferently
166 (Barsoum et al. 2015) or negative mixture effects were observed (Nothdurft and Engel 2020).
167 However, interactions between a given pair of species are often dynamic, changing as
168 resource availability and climate conditions change. It is not unusual for net complementary
169 interactions between a given species pair to transform into net competitive interactions, or
170 vice versa (Forrester 2014, Jacobs et al. 2022).

171 At the individual tree level, species coexistence is driven by fine-scale spatial
172 patterns and the competitive ability of species (Collet et al. 2017). Even if species are mixed
173 at the stand scale, species may be segregated at the local scale. Such fine-scaled spatial
174 patterns may be captured by local competition indices and describe the physiological response
175 of trees in the interspecific and intraspecific neighbourhood (Höwler et al. 2019). Local
176 heterogeneity may also result from small-scale spatial heterogeneity of environmental factors
177 (micro-site) or interactions between species. Such local competition effects are rarely
178 included in tree-ring studies.

179 **Hypothesis**

180 In this study we analyse the climate-growth relationship of *Quercus spp.* and *P. sylvestris*
181 along a gradient across Europe in monospecific and mixed stands. We hypothesize that:

- 182 (1) Tree growth reactions are site-specific. (i) Trees within the same bio-climatic regions
183 show analogous tree growth patterns while patterns between different bio-climatic
184 regions differ.
- 185 (2) Tree growth reactions to drought are species, mixture and season specific (i) *Q. spp.* is
186 more drought resistant (ii) *P. sylvestris* is more tolerant to cold, (iii) both species react
187 more sensitively to drought on drought prone sites (iv) both species react less sensitive
188 to drought in mixture compared to monocultures
- 189 (3) Tree growth is influenced by mixture (i) mixture effects are positive for both tree
190 species, (ii) mixture effects depend on local competition

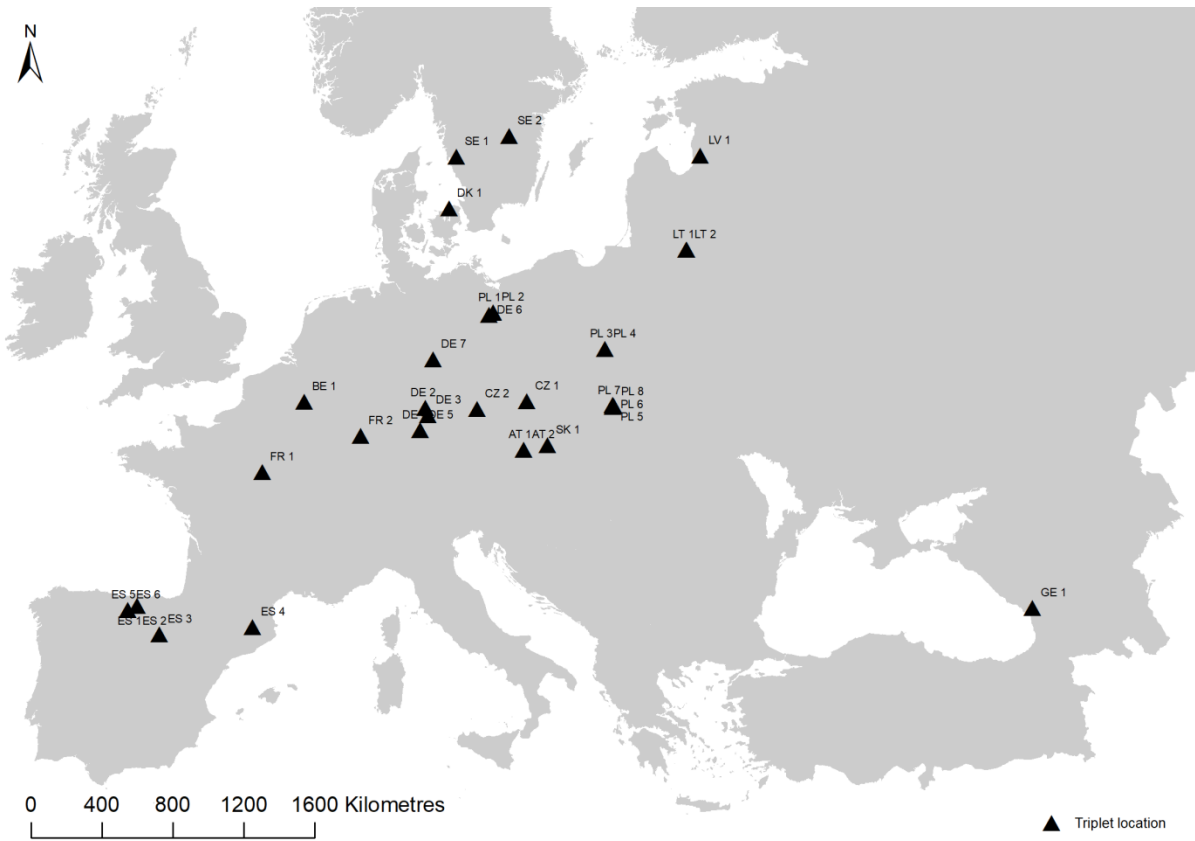
191

192 **2. Material and Methods**

193 **2.1 Material**

194 2.1.1 Study area and research sites

195 This study builds on a comprehensive transect of 36 *Q. spp.* - *P. sylvestris* triplets
196 located along an ecological gradient through Europe, reaching from nutrient-poorer and xeric
197 to nutrient-richer and mesic sites (Fig. 1). The transect was initially established as part of the
198 ERA-Net SUMFOREST project REFORM (“Resilience of FOrest Mixtures”, reform-
199 mixing.eu) and is described in detail in previous studies focusing on stand productivity and
200 tree drought resilience (Steckel et al. 2019, Pretzsch et al. 2020, Steckel et al. 2020a). Long-
201 term mean temperature on triplets ranged between 5.5 °C and 11.5 °C, with long-term mean
202 precipitation ranging from 456-929 mm (Table 1). By design, each triplet contains three sub-
203 plots, representing one mixed *P. sylvestris* - *Q. spp.* stand and two monospecific stands of
204 each species, respectively. In the sampling protocol stands were required to be even-aged, at
205 maximum density and unthinned for at least 20 years and exhibit a more or less pronounced
206 mono-layered structure. Stand age and stand density are given in Table 1.



208

209 **Figure 1** Triplets (*Q. spp.-P. sylvestris*) distribution along European ecological gradient

210 **Table 1** Summary statistics of triplets. Tri = Triplet code; Lat = Latitude (degree); Long = Longitude (degree);
 211 Incl=Inclination (degree); Asp=Aspect (degree); P = long-term mean (1976-2015) annual precipitation (mm);
 212 T = long-term mean (1976-2015) annual temperature (Celsius degree); n = number of year rings observed on
 213 each plot; Age = Mean age of cored trees; QMD = quadratic mean diameter (cm); SDI = Stand density index for
 214 pure *Quercus spp.* (*Q.*) plots, pure *Pinus sylvestris* (*P.*) plots and mixed (*M.*) plots; id = average yearly diameter
 215 increment (mm) for *Quercus spp.* (*Q.*) and *Pinus sylvestris* (*P.*) in pure and mixed stands in the 20 years
 216 analysed; Note that one triplet was not included because no trees were available, were local competition
 217 variables could be calculated without edge effect

Tri	Lat	Long	Incl	Asp	P	T	n	Age	QMD	SDI			id			
										Q.	P.	M.	Pure		Mixed	
													Q.	P.	Q.	P.
AT 1	48.6	15.8	0.0	180	658	8.7	1452	103	30.5	556	1024	785	0.266	0.150	0.177	0.161
AT 2	48.6	15.8	0.0	180	658	8.7	1249	56	26.3	643	1152	876	0.222	0.229	0.209	0.207
BE 1	50.2	4.7	0.0	180	929	9.3	1298	69	26.0	413	477	534	0.265	0.459	0.318	0.332
CZ 1	50.2	16.0	0.0	180	620	9.2	1012	95	26.2	632	900	962	0.225	0.176	0.207	0.195
CZ 2	49.9	13.5	0.0	180	573	8.7	726	76	21.2	937	1327	1053	0.235	0.250	0.178	0.327
DE 1	49.9	10.8	28.8	225	615	8.5	1122	108	27.5	1049	1034	1045	0.217	0.200	0.206	0.221
DE 2	49.9	10.8	27.6	225	615	8.5	858	108	26.4	1007	1060	1168	0.179	0.215	0.257	0.163
DE 3	49.7	11.0	23.6	315	663	8.4	22	110	29.7	836			0.092			
DE 4	49.2	10.6	6.4	180	718	8.1	748	48	20.0		1144	921		0.219	0.541	0.440
DE 5	49.2	10.6	4.8	180	718	8.1	1078	46	20.7	864	1076	879	0.470	0.325	0.525	0.510
DE 6	52.9	14.1	0.0	180	558	9.4	1496	82	30.0	765	897	816	0.336	0.306	0.301	0.396
DE 7	51.5	11.2	53.2	202	503	9.5	946	80	21.0	1459	1715	1429	0.251	0.114	0.187	0.191
DK 1	56.0	12.1	0.0	180	667	8.0	462	50	27.1	833	1014	795	0.330	0.321	0.409	0.550
ES 1	43.0	3.8	45.3	236	819	11.4	503	45	20.6	1210	1517	1526	0.114	0.343	0.243	0.273
ES 2	43.0	3.8	41.9	259	819	11.4	374	45	21.5	1126	1461	1513	0.214	0.451	0.288	0.199
ES 3	42.0	2.0	27.0	180	586	10.0	660	61	24.9	911	1158		0.152	0.503		
ES 4	42.3	2.1	60.7	22	846	10.9	861	53	17.9	637	395		0.143	0.312		
ES 5	42.9	4.2	26.4	45	793	9.9	902	55	25.4	1258	1444	1412	0.206	0.373	0.259	0.310
FR 1	47.8	2.5	0.0	180	724	11.0	1332	64	28.7	651	867	705	0.288	0.361	0.246	0.319
FR 2	49.0	7.5	25.4	45	893	9.8	1496	112	37.3	413	792	519	0.296	0.190	0.255	0.185
GE 1	43.0	41.6	15.1	79	456	11.5	532	83	21.0	608	694	1419	0.130	0.189	0.174	0.333
LT 1	54.8	24.1	0.0	180	614	6.6	792	59	26.7	1093	632	871	0.349	0.290	0.242	0.298
LT 2	54.8	24.1	0.0	180	614	6.6	968	86	31.3	811	927	864	0.270	0.254	0.295	0.367
LV 1	57.5	24.8	0.0	180	657	5.5	1254	70	28.9	565	835	801	0.196	0.304	0.181	0.430
PL 1	53.0	14.3	10.4	180	604	9.1	946	55	23.1	863	1071	1054	0.240	0.333	0.254	0.374
PL 2	53.0	14.3	7.4	180	604	9.1	1034	56	24.2	899	1086	901	0.230	0.301	0.237	0.397
PL 3	51.8	19.9	0.0	180	554	8.1	1100	74	29.7	893	905	880	0.211	0.362	0.355	0.354
PL 4	51.8	19.9	0.0	180	554	8.1	1144	75	31.3	808	944	750	0.304	0.329	0.419	0.404
PL 5	50.1	20.3	0.0	180	671	8.4	1716	65	29.0	845	1020	999	0.287	0.352	0.421	0.323
PL 6	50.1	20.3	0.0	180	671	8.4	1606	65	29.5	854	1155	907	0.291	0.378	0.327	0.340
PL 7	50.0	20.4	0.0	180	680	8.4	1705	75	36.2	747	1218	804	0.452	0.282	0.357	0.298
PL 8	50.0	20.4	0.0	180	680	8.4	858	85	39.2	763	868		0.260	0.266		
SE 1	57.5	12.4	6.0	202	891	7.2	962	86	26.2	505	883	568	0.336	0.199	0.380	0.322
SE 2	58.0	15.6	38.1	169	598	6.0	738	127	27.4	876	1149	876	0.147	0.088	0.155	0.096
SK 1	48.7	17.1	0.0	180	580	9.8	814	66	27.6	678	1051	728	0.166	0.202	0.182	0.220

218

219

220 2.1.2 Data collection and preparation

221 Field sampling was carried out in late 2017 at the end of the growing season,
222 following a comprehensive standardized sampling protocol (Pretzsch et al. 2020). All trees on
223 each plot of the triplets were assessed and for each tree coordinates, dbh, height and height to
224 the crown base were recorded. On a sub-sample of trees, two increment cores were extracted
225 at breast height (1.3 m) from north and east cardinal directions, covering the entire diameter
226 distribution. A minimum of 20 dominant and 10 sub-dominant trees per species were sampled
227 on each plot, after removing damaged cores and trees sampled close to plot boundary, to
228 avoid edge effects in the calculation of local competition (see section 2.2.1 neighborhood
229 analysis), the resulting number of cores was 785 and 804 trees for *Q. spp.* and *P. sylvestris*,
230 respectively for the total gradient. The diameter at breast height (dbh) was also measured with
231 an accuracy of 0.1 cm, using a girth tape.

232 Annual ring-widths were measured from each increment core, using standardized
233 dendrochronological techniques (Speer 2010). Cross-dating was performed for the individual
234 plots of each triplet, guided by narrow ring widths in species-specific pointer years
235 (Schweingruber et al. 1990). Inter-series correlation ranged between 0.34-0.77 for *Q. spp.* and
236 0.39-0.74 for *P. sylvestris*. The expressed population signal, estimating how well the
237 particular sample of cores at hand represents the theoretical population chronology from
238 which it is drawn based on the inter-series correlation (Wigley et al. 1984), ranged from 0.61-
239 0.96 and 0.84-0.99 for *Q. spp.* and *P. sylvestris*, respectively. Thus, it was above the
240 recommended threshold value of 0.85 for *P. sylvestris* on all sites, but below this threshold on
241 some sites for *Q. spp.*. To reflect the current competitive status, only year-ring series from
242 1996-2017, a period with no silvicultural interventions, were used in this analysis.

243

244 2.1.3 Climate data

245 Meteorological information (monthly mean temperature (T) and monthly
246 precipitation total (P)) was obtained from local meteorological stations. It was assumed that
247 the observations from meteorological stations reflect local site conditions as well as possible.
248 Meteorological stations used were located in close proximity to the research sites in question.
249 Such sites did not exhibit any regional topographical peculiarities that would prohibit such an
250 approach.

251 In cases where no suitable local station data was available (no coverage at all or
252 distance to site considered too far), interpolated observations as gridded data sets as provided
253 by national meteorological services or the CRU (Climatic Research Unit) 0.5° (Harris et al.
254 2020). In general, such modelled data used was cross-checked with station measurements
255 (where possible) to evaluate the comparability of data sources. Monthly meteorological
256 data were subsequently further aggregated to annual values or multi-annual means. From the
257 gridded temperature and precipitation data, the potential evapotranspiration (PET) according
258 to Thornthwaite (1948) and the climatic water balance (P-PET) were derived for each month.
259 In addition, different drought indices were calculated: the De Martonne aridity index (DMI)
260 (Martonne 1926), the standardized precipitation index (SPI) (McKee et al. 1993), and the
261 standardized precipitation and evapotranspiration index (SPEI) (Vicente-Serrano et al. 2010).
262 The climate growth relationship was analyzed from August of the previous year to September
263 of the year of tree-ring formation based on previous dendroecological and intra-annual growth
264 studies (e.g. Sánchez-Salguero et al. 2013).

265

266 **2.2 Methods**

267 2.2.1 Neighbourhood analysis

268 We analyzed the competitive constellation of every cored tree on the plot to reveal
269 how the local inter- and intra-specific environment modify tree growth. First, a circle with the

270 recommended radius of $r = 7$ m (Biging and Dobbertin 1992, Biging and Dobbertin 1995)
271 around the stem coordinate of each cored tree was constructed and all trees within the circle
272 were used in the neighbourhood analyses. Circles of this size include 8-9 trees on average and
273 at least the 5–6 most impactful neighbors (Prodan 1968a, Prodan 1968b).

274 For the neighbourhood analysis, we calculated the tree's specific competition index
275 according to Hegyi (1974), with $ci_j = \sum_{i \neq j}^n \left(\frac{d_i}{d_j} \times \frac{1}{dst_{ij}} \right)$, which quantifies the competition of
276 central tree j based on its stem diameter (d_j), the stem diameters of its neighbours (n) $d_{i,i=1...n}$,
277 and the distance (dst_{ij}) between the central tree j and the respective neighbors and the local
278 Stand Density Index, SDI, (Reineke 1933): $SDI = N \times \left(\frac{25}{d_g} \right)^\alpha$, where N is the stem number
279 within the 7 m radius, d_g is the quadratic mean diameter within the radius and α is the
280 species-specific allometric exponent derived by Pretzsch and Biber (2010). We used the same
281 approach to calculate the tree's specific density, but did not include the tree of interest (central
282 tree).

283 The trees sampled in the circle were also used to calculate the local mixing
284 proportions using all admixed tree species. The mixing proportions $m_1 \dots m_n$ should reflect
285 the area proportions of the two or more species in the observed mixed stands (Dirnberger et
286 al. 2017, Pretzsch and Del Río 2020). Tree number, basal area or volume proportions are only
287 appropriate for this purpose if the mixed species have similar growing area requirements
288 (Pretzsch et al. 2017, pp. 137-140). The considered tree species vary per se in the growing
289 area requirement and maximum stand density in fully stocked stands. In order to standardize
290 the density and to calculate unbiased area related to mixing proportions we applied the
291 equivalence factors by Pretzsch and Biber (2016). The potential edge effect was considered
292 by simply removing all trees with search radii reaching beyond the edge of the plots.

293 To describe forest structure, the Gini coefficient by basal area was calculated in the
294 local neighborhood with a radius of 7 m as suggested by Binkley et al. (2006). Furthermore,

295 the relative dbh was calculated by dividing individual tree dbh by quadratic mean diameter
296 (dg) averaged over all species in the stand to characterize each tree's social position at the
297 stand level.

298

299 2.2.1 Modeling

300 Diameter increment was modeled using the generalized additive models (GAMs),
301 originally developed by Hastie and Tabshirani (1990) blending properties of additive models
302 with generalized linear models. In generalized additive models, the expected value depends
303 on unknown smooth functions of the predictor variables and the observed values are assumed
304 to be of some exponential family distribution (Wood 2011, 2017).

305 GAMs were estimated using the mgcv-package (Wood 2011, 2017) in R (R Core
306 Team 2018); Within the GAM-framework of mgcv, model-covariates may be specified: (a) in
307 parametric form or (b) non-parametrically, as smooth functions. The smooth functions are
308 made of basis functions, that added together compose the smooth terms, hence the name
309 (Wood 2011, 2017). Each smooth f_j is represented by a sum of k simpler, fixed basis
310 functions ($b_{j,k}$). multiplied by corresponding coefficients $\beta_{j,k}$ which need to be estimated.

$$311 \quad f_j(x_j) = \sum_{k=1}^k (\beta_{j,k} \cdot b_{j,k}(x_k)) \quad (1)$$

312 Numerous different basis functions, such as cubic splines, circular splines or thin plate
313 regression splines, are provided by the mgcv-package, and the type and number of basis
314 functions can be set.

315 Given a matrix of known coefficients S , we can formally note a penalized likelihood function:

$$l_p(\beta) = l(\beta) - \frac{1}{2} \sum_j \lambda_j \beta^T S_j \beta$$

316 Where $l(\beta)$ is the usual GLM likelihood function and λ_j are the smoothing parameters. The
317 part of the function including λ penalizes curvature in the function and
318 controls the degree to which the model fits the data. As $\lambda \rightarrow \infty$, the estimator for f_j becomes
319 linear while $\lambda = 0$ would allow any f that interpolates the data (Wood, 2006). Technically, it
320 can be set, but it is usually determined programmatically by minimizing the least squares
321 criterion subject to a roughness penalty based on second derivatives, i.e. if the second
322 derivatives are zero, the function is linear and these departures from linearity (smoothness)
323 are penalized, which avoids overfitting. The final complexity of the smooth is given by the
324 effective degree of freedom (edf) and an edf of 1 is equivalent to a linear function. The model
325 degrees of freedom are obtained by summing the effective degrees of freedom (Wood 2011,
326 2017).

327

328 In addition, the mgcv-package also allows for the inclusion of random terms. Since the
329 data set used in this study is a hierarchical data set with trees at the same plot and
330 measurements at the same tree being correlated, random effects at the tree, triplet and year
331 level for both intercept and slope were included, where necessary. Diameter increment was
332 linked to the covariates with a logarithmic link function and as exponential family
333 distribution, the Tweedie distribution was used, which allows for fitting the type of
334 exponential distribution from the data via a parameter p , encompassing different exponential
335 distributions such as the normal ($p=0$), Gamma ($p=2$) and inverse Gaussian distribution.
336 Parametric terms were used for categorical covariates, whereas smooth functions were used
337 for continuous covariates, with thin plate regression splines as basis functions. The number of
338 basis functions used in model fitting was 10. The mgcv option “select” was set to TRUE,
339 enabling shrinkage. Shrinkage adds an extra penalty and if the smoothing parameter λ , is
340 large enough, the coefficients will shrink to zero. In this manner it can be assessed whether a
341 predictor is adding anything to the model and it can be used as variable selection technique.

342 Enabling shrinkage helps to deal with concurvity of the covariates (Marra and Wood 2011).
343 Concurvity refers to the non-linear dependence of covariates in the GAM-framework, causing
344 unstable estimates similar to collinearity in the linear case. Interactions were included as
345 tensor product interactions, which can be used for variables that operate on different scales.
346 The specification “ti-interaction”, i.e. a tensor product interaction where variable 1, variable 2
347 and their combination are separate, was used. All covariates described in the data section were
348 included in model fitting and the best fitting model was selected based on Akaike’s
349 information criterion (AIC) (Akaike 1973). From the fitted model variance components for
350 smoothing parameters and random effects were extracted. Note the two variance components
351 for the tensor product smooth indicated by “ti”. The first is the variance component of the
352 tensor product smooth for the marginal basis of the first variable; the second is the variance
353 component of the tensor product smooth for the marginal basis of the second variable.

354

355 **3. Results**

356 **3.1 Overall model results**

357 The final fitted models for diameter increment for *P. sylvestris* and *Q. spp.* included
358 mixture effects at the plot level, age, relative dbh, local SDI, tree species specific Gini
359 coefficient, long-term mean temperature, evapotranspiration of the month of September of the
360 previous year and for each month from April-July (PET 4-7) of the current year and the
361 interaction thereof with relative dbh as fixed effects and triplet and tree specific random
362 effects (Equation 2). The climatic drivers differed slightly between species; PET in April
363 (PET 4) was significant for *P. sylvestris* only, PET in May (PET 5) for *Q. spp.*. The
364 interactions between climate and stand density index and climate and mixture were not
365 significant.

366 $\ln(id_{ijk}) =$
367 $\beta_o + \beta_1 \cdot mixture + f(age) + f(local\ SDI) + f(gini\ ba) + f(relative\ dbh) +$
368 $f(LTMT) + f(PET\ previous\ 9) + f(PET\ 4 - 7) + f(PET\ previous\ 9,\ relative\ dbh) +$
369 $f(PET\ 4 - 7,\ relative\ dbh) + \gamma_{1i} \cdot Triplet \cdot t_{ij} + \gamma_k \cdot Tree_k + y_k \cdot Tree_k \cdot f(age) + e_{ijk}$
370 (2)
371

372	id_{ijkl}	observed diameter increment for tree k, in season j, on triplet i
373	β_o	population mean of diameter increment
374	$\beta_1 \cdot mixture$	parametric mixture effect
375	$f(age)$	smooth function for age
376	$f(local\ SDI)$	smooth function for local SDI
377	$f(gini\ ba)$	smooth function for species specific Gini coefficient
378	$f(relative\ dbh)$	smooth function for relative dbh
379	$f(LTMT)$	smooth function for long-term mean temperatures
380	$f(PET\ previous\ 9)$	smooth function for monthly potential evapotranspiration for
381		September of the previous year
382	$f(PET4-7)$	smooth function for monthly potential evapotranspiration for
383		each month from April - July
384	$\gamma_{1i} \cdot Triplet \cdot t_{ij}$	triplet and year specific random effect
385	$\gamma_k \cdot Tree_k$	tree specific random intercept
386	$y_k \cdot Tree_k \cdot f(age)$	tree specific random slope, random effect of age within each
387		level of tree
388	e_{ijk}	random error
389		

390 Overall, the model explained 87.4 % and 87.0 % of the total variation for each of the
391 two models (Table 2). Thereof, 41.9 % and 38.2 % were explained by the fixed part of the
392 model for *Q. spp.* and *P. sylvestris*, respectively. The most important variables in the fixed
393 part of the model were relative dbh, species-specific Gini coefficient, and long-term mean
394 temperature for *Q. spp.* and relative dbh as indicated by the variance components (Table 3). In
395 the random part of the model, tree-specific random effects explained more variation, than
396 triplet- and year-specific random effects (Table 3).

397 For the parametric mixture effects the coefficient and the p-value are given; Table 2
398 contains the effective degrees of freedom and the p-value for the smooth terms. A high degree
399 of non-linearity for the fixed part of the model was found for age, relative dbh, and local SDI
400 whereas a linear decrease, as is indicated by effective degrees of freedom of 1, was found for
401 other variables, in particular for PET in various month for *P. sylvestris*.

402 **Table 2:** Coefficients for parametric effects (Estimate) and effective degrees of freedom for smooth terms (edf)
403 for *Quercus spp.* and *Pinus sylvestris*. The p-value indicates significance of terms. R², Akaike's information
404 criterion and the number of observations are given in the bottom lines. Tweedie p gives the estimate for the

405 shape parameter p of the Tweedie distribution. Note that mixture and LTM are not significant in the *Quercus*
 406 *spp.* model and PET in May is not significant in the *Pinus sylvestris* model as is indicated by the italic font.
 407 Variables modelled as random effects are indicated in bold letters

Variable	<i>Quercus spp.</i>		<i>Pinus syl.</i>	
	Estimate	p.value	Estimate	p.value
Intercept	-1.66	0.000	-2.03	0.000
Mixture	<i>0.05</i>	<i>0.574</i>	0.24	0.030
Variable	edf	p.value	edf	p.value
s(age)	7.53	0.000	6.80	0.000
s(local SDI)	6.08	0.000	7.83	0.000
s(rel. dbh)	6.28	0.000	6.95	0.000
s(Gini coefficient)	4.32	0.010	6.12	0.004
s(LTM temp)	<i>2.44</i>	<i>0.057</i>	1.00	0.020
s(PET Sept. prev)	1.79	0.000	4.45	0.003
s(PET April)	-	-	1.00	0.001
s(PET May)	2.37	0.000	<i>1.00</i>	<i>0.100</i>
s(PET June)	1.67	0.000	1.28	0.001
s(PET July)	2.04	0.000	3.66	0.000
s(PET April, rel. dbh)	-	-	6.01	0.010
s(PET July, rel. dbh)	7.23	0.000	-	-
s(PET Sept, prev. rel.dbh)	5.06	0.000	-	-
s(Tree ID)	641.94	0.000	700.33	0.000
s(Tree ID, age)	653.24	0.000	706.16	0.000
s(Triplet, Year)	645.99	0.000	641.47	0.000
R ²	0.874		0.870	
AIC	-52605.71		-47896.73	
n	16696		17284	
Tweedie (p)	1.651		1.347	

408
 409

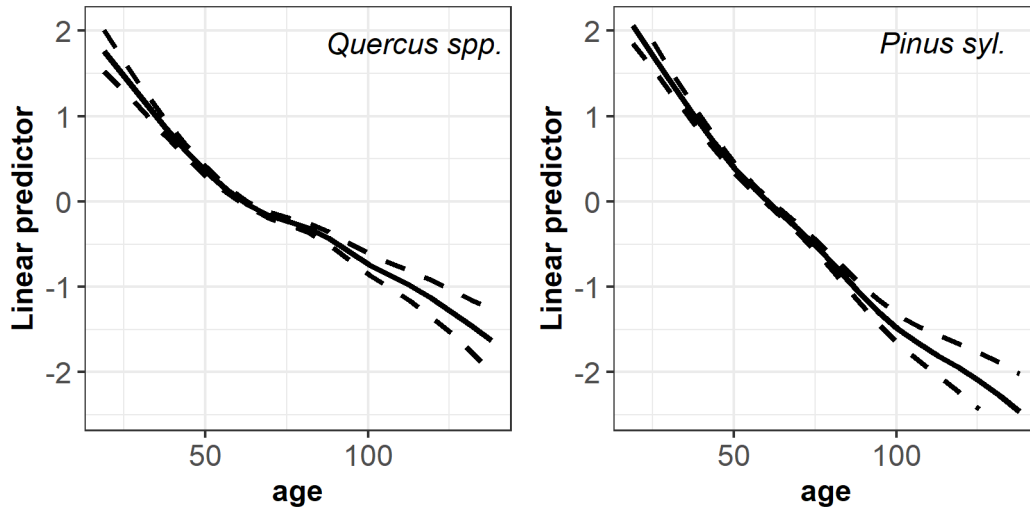
410 **Table 3:** Variance components (as standard deviation) and their upper and lower confidence limits for the
 411 models of *Quercus spp.* and *Pinus sylvestris*. Note the two variance components for the tensor product smooth
 412 indicated by ti. The first is the variance component of the tensor product smooth for the marginal basis of the
 413 first variable, the second is the variance component of the tensor product smooth for the marginal basis of the
 414 second variable. Variables modelled as random effects are indicated in bold letters.

Variable	<i>Quercus spp.</i>			<i>Pinus sylvestris</i>		
	std.dev	lower	upper	std.dev	lower	upper
s(age)	0.0031	0.0016	0.0064	0.0026	0.0014	0.0049
s(local SDI)	0.0000	0.0000	0.0000	0.0000	0.0000	0.0001
s(rel. dbh)	0.8516	0.1435	5.0527	0.9739	0.9736	0.9742
s(Gini coefficient)	1.9878	1.1261	3.5090	4.4684	2.3557	8.4760
s(LTM temp)	0.1728	0.0115	2.6057	0.0003	0.0000	1069e+107
s(PET Sep. prev)	0.0004	0.0001	0.0012	0.0024	0.0000	0.0101
s(PET April)	-	-	-	0.0000	0.0000	1055e+263
s(PET May)	0.0006	0.0000	0.0133	0.0000	0.0000	0.0033
s(PET June)	0.0003	0.0000	0.0021	0.0002	0.0001	0.0005
s(PET July)	0.0003	0.0001	0.0012	0.0010	0.0003	0.0033
ti(PET Sep. prev, rel. dbh)1	0.0201	0.0054	0.0749	-	-	-
ti(PET Sep. prev, rel. dbh)2	0.0014	0.0013	0.0015	-	-	-
ti(PET April, rel. dbh)1	-	-	-	0.0083	0.0028	0.0248
ti(PET April, rel. dbh)2	-	-	-	0.0248	0.0043	0.0049
ti(PET July, rel.dbh)1	0.0087	0.0032	0.0235	-	-	-
ti(PET July, rel.dbh)1	0.0093	0.0009	0.0934	-	-	-
s(Tree ID)	1.0398	0.9760	1.1077	1.3867	1.3078	1.4704
s(Tree ID , age)	0.0161	0.0152	0.0171	0.0220	0.0208	0.0234
s(Triplet , Year)	0.1580	0.0895	0.2789	0.1761	0.0928	0.3340
Residual	0.1517	0.1494	0.1540	0.1350	0.1330	0.1370

415

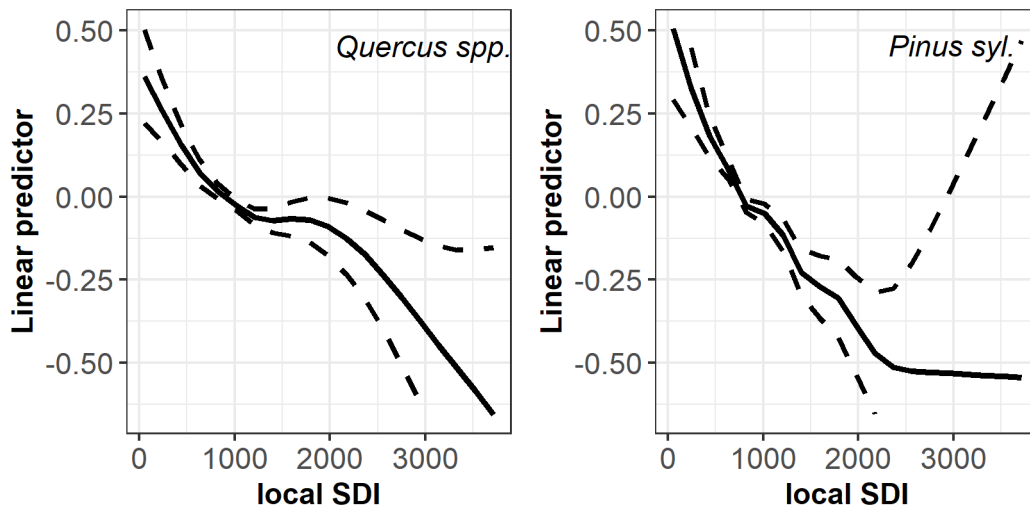
416 3.2 Fixed effects – parametric and smooth terms

417 The species mixture increased diameter increment for both *Q. spp.* and *P. sylvestris*
 418 (Table 2), but the effect was significant for *P. sylvestris* only. Both tree species showed a
 419 decrease in diameter increment with age (Fig. 2) and local SDI (Fig. 3). the decrease being
 420 sharper for *P. sylvestris* than for *Q. spp.* (Fig. 2,3). Confidence intervals were narrow for age
 421 for the total range of values, but became very large for high SDI values.



422

423 **Figure 2:** Effect of age on diameter increment for *Quercus robur* and *Quercus petraea* (left) and *Pinus sylvestris*
 424 (right). Solid line: prediction, dashed lines: confidence interval. Note that the linear predictor ($\ln(\text{diameter}$
 425 increment)) is zero at the mean of the covariate age.
 426
 427



428

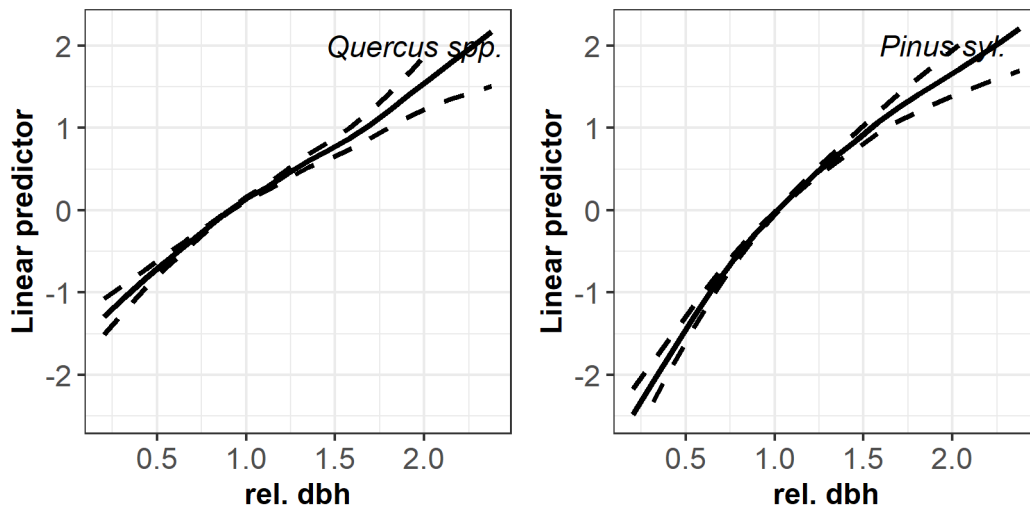
429 **Figure 3:** Effect of local SDI on diameter increment for *Quercus robur* and *Quercus petraea* (left) and *Pinus*
 430 *sylvestris* (right). Solid line: prediction, dashed lines: confidence interval. Note that the linear predictor
 431 ($\ln(\text{diameter increment})$) is zero at the mean of the covariate local SDI.
 432

433 Both species showed an almost linear increase in diameter increment with relative
 434 dbh; Thus trees in the stand upper layer had higher increment rates (Fig. 4).

435

436

437



438

439 **Figure 4:** Effect of relative dbh (dbh divided by quadratic mean diameter) on diameter increment for *Quercus*
 440 *robur* and *Quercus petraea* (left) and *Pinus sylvestris* (right). Solid line: prediction, dashed lines confidence
 441 interval. Note that the linear predictor ($\ln(\text{diameter increment})$) is zero at the mean of the covariate relative
 442 dbh.
 443

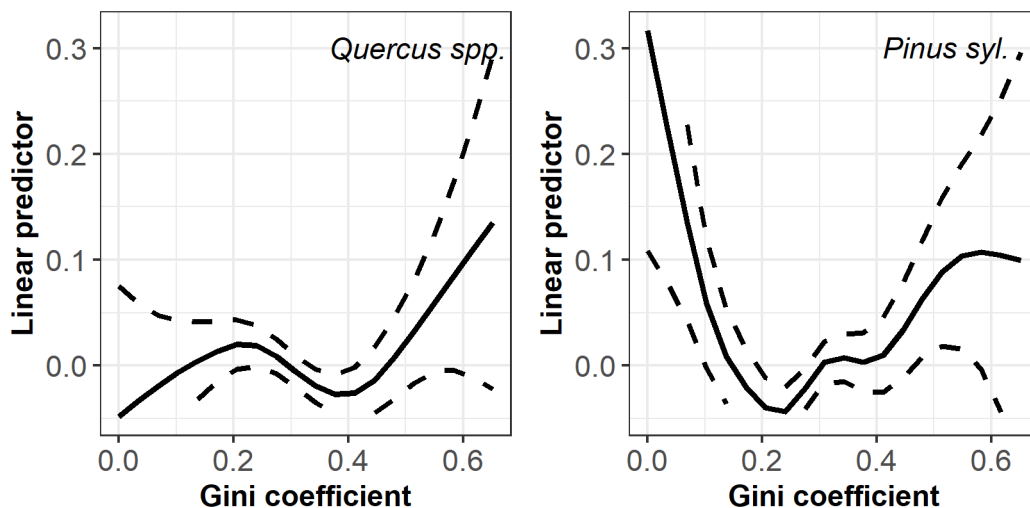
444

Non-linear patterns were observed for the relationship between Gini coefficient and

445 diameter increment and the patterns for the two tree species differed (Figure 5). It might

446 point to the fact, that this variable captures different tree structures in the observed data,

447 but that this pattern might not be generalizable.



448

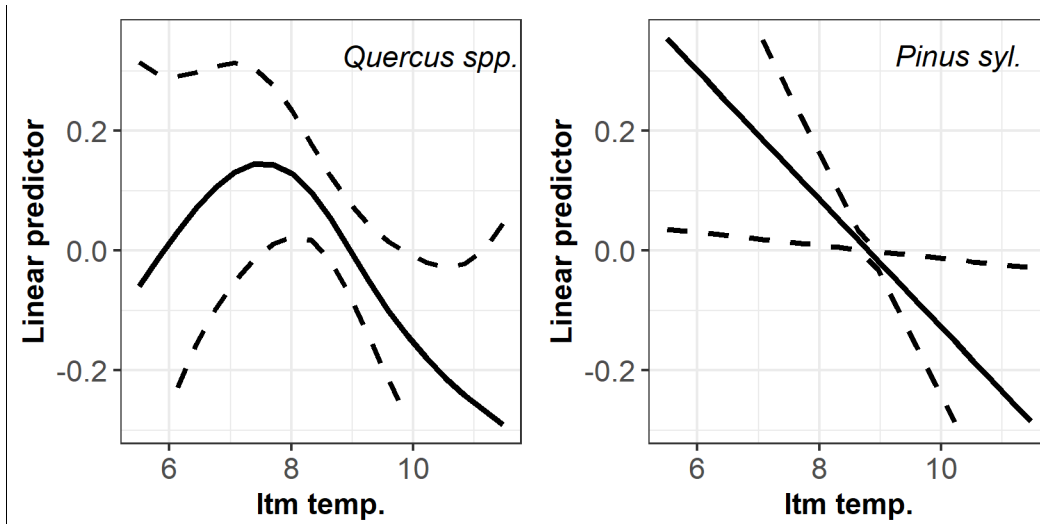
449 **Figure 5:** Effect of Gini coefficient on diameter increment for *Quercus robur* and *Quercus petraea* (left) and
 450 *Pinus sylvestris* (right). Solid line: prediction, dashed lines confidence interval. Note that the linear predictor
 451 ($\ln(\text{diameter increment})$) is zero at the mean of the covariate Gini coefficient.
 452

453

The effect of long-term mean temperature for both tree species is illustrated in Fig. 6,

454 but the effect was significant for *P. sylvestris* only. Effects differed for the two tree species:

455 the growth of *Q. spp.* indicated an optimum temperature at 7° C, but the *P. sylvestris* growth
 456 showed a linear decrease with temperature (Fig. 6). Both relationships have very large
 457 confidence intervals.



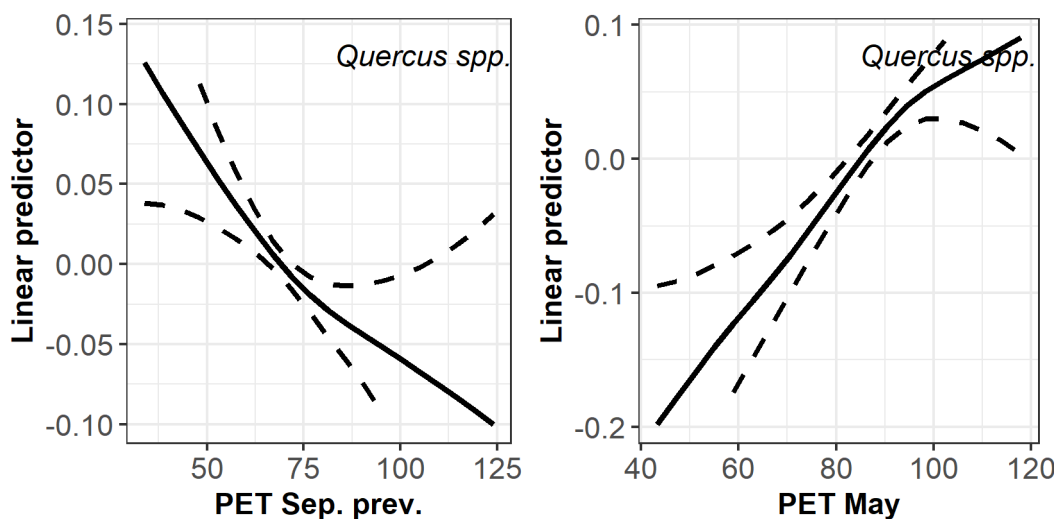
458

459 **Figure 6:** Effect of long-term mean temperature (lrm temp.) from the years 1976-2015 on diameter increment
 460 for *Quercus robur* and *Quercus petraea* (left) and *Pinus sylvestris* (right). Solid line: prediction, dashed lines
 461 confidence interval. Note that the p-value for *Q. spp.* is 0.1. Note also that the linear predictor ($\ln(\text{diameter}$
 462 increment)) is zero at the mean of the covariate lrm temp. The relationship between the linear predictor and
 463 lrm temp. is linear and could also be represented by a parametric linear term.

464

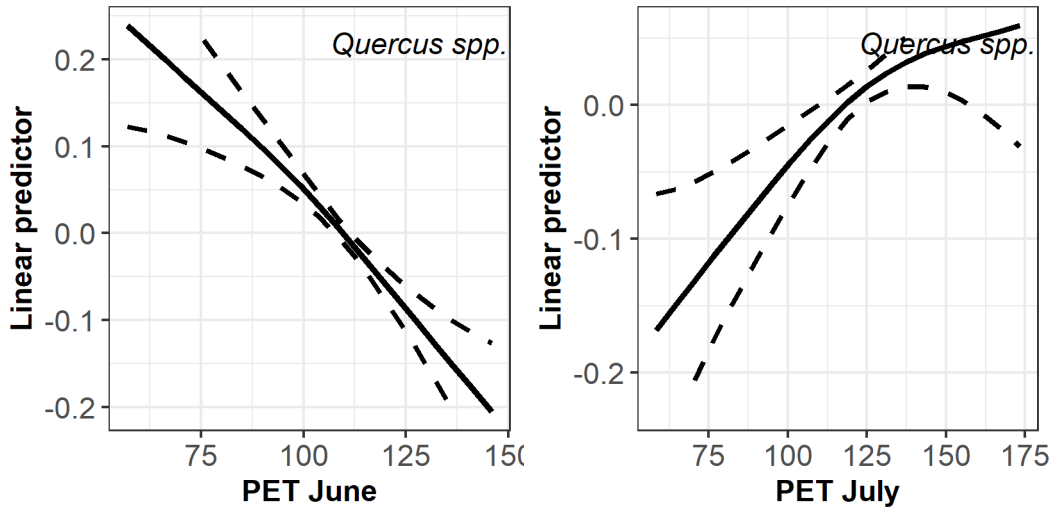
465 In addition to long-term mean temperature, both species responded to
 466 evapotranspiration in different months. In general, autumn of the previous year and spring and
 467 summer of the current year influenced tree growth. Influential months differed between
 468 species. For both species, the influential months were September of the previous year and
 469 June and July of the current year (Fig. 7, Fig. 8); An additional month of the current year had
 470 also a significant influence: May for *Q. spp.* and April for *P. sylvestris*. Patterns significantly
 471 differed between months and often showed opposite trends. The diameter increment showed a
 472 decrease with increasing PET of September of the previous for *Q. spp.* and was highly non-
 473 linear for *P. sylvestris*. In spring, at the onset of growth, tree growth increased with increasing
 474 PET for both species, which switched to a sharp decrease in June. Note the very different
 475 scales of observed PET values on the x-axis for various months and the different scale for the
 476 linear predictor. A larger effect of climate on diameter increment was observed in spring

477 compared to autumn, but effects for both tree species had a similar magnitude for the same
478 month. June is the most influential month for both tree species. Interactions of PET with
479 relative dbh were significant for September of the previous year and July of the current year
480 for *Q. spp.* (Fig. 9) and with PET in April of the current year for *P. sylvestris* (Fig. 10). The
481 climate-growth relationship shown in the figures (Fig. 9, Fig. 10) differs for trees of different
482 social position (the most dominant and suppressed trees) in particular at the beginning and the
483 end of the growing season. These are the only significant interactions at the logarithmic scale
484 of diameter increment. Such interactions are, however, significant for all months, when
485 modelling diameter increments on a linear scale; As the fit of a concurrent linear model
486 showed, different social classes behave differently to the climate in a specific month.

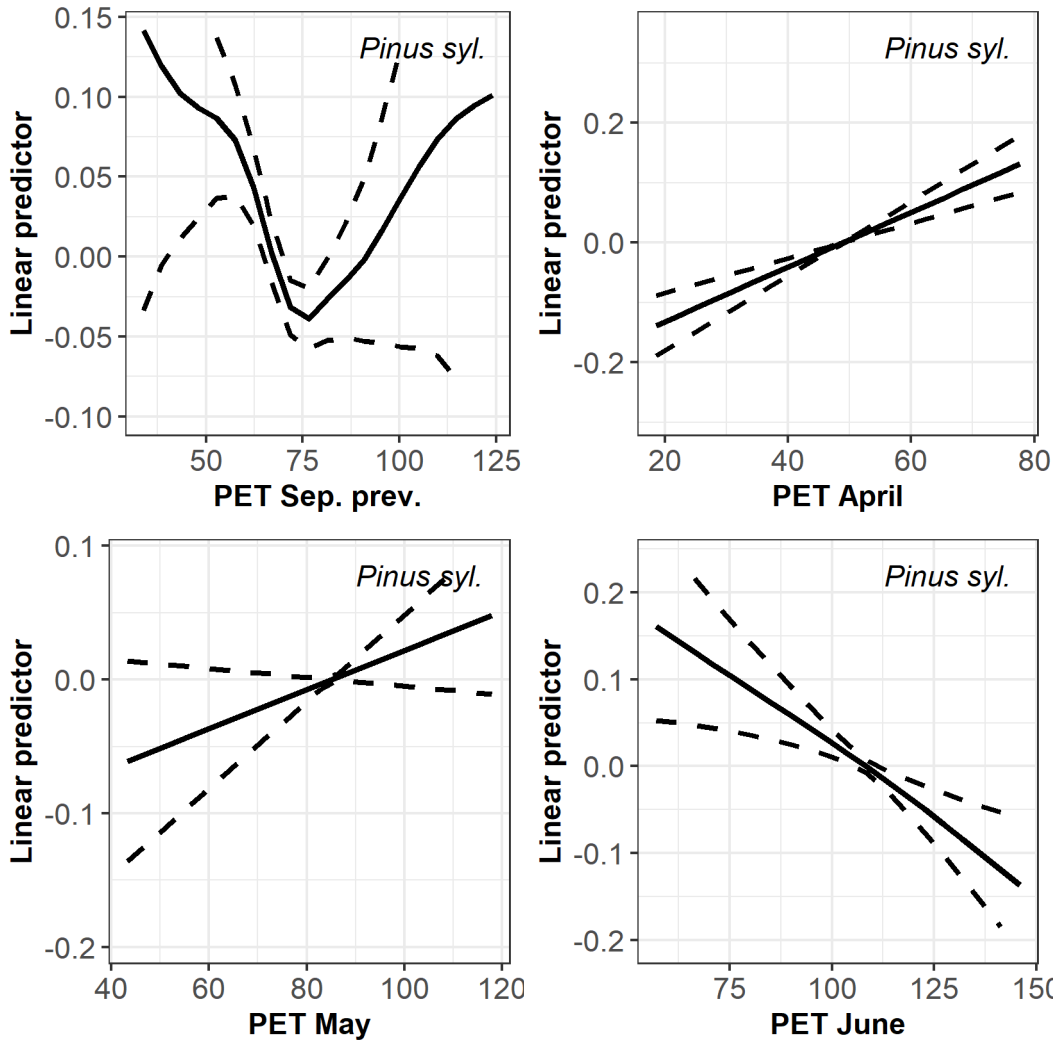


487

488

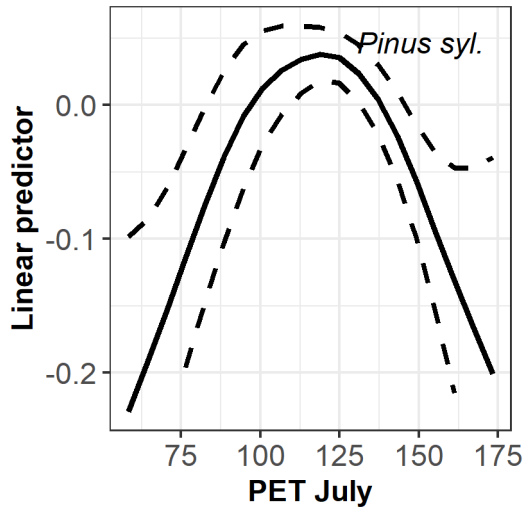


489
 490 **Figure 7:** Effect of potential evapotranspiration (PET) in the month of September of the previous year and
 491 April–July of the current year on diameter increment for *Quercus robur* and *Quercus petraea*. Solid line:
 492 prediction, dashed lines confidence interval. Note that the linear predictor ($\ln(\text{diameter increment})$) is zero at
 493 the mean of the covariate PET in the respective month.



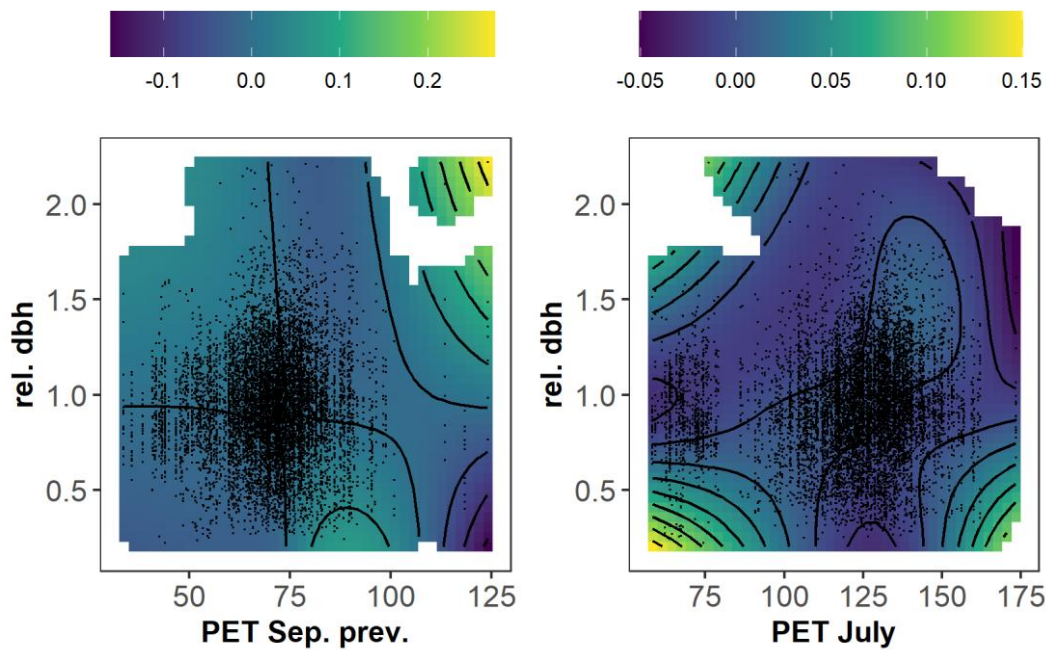
495

496
 497



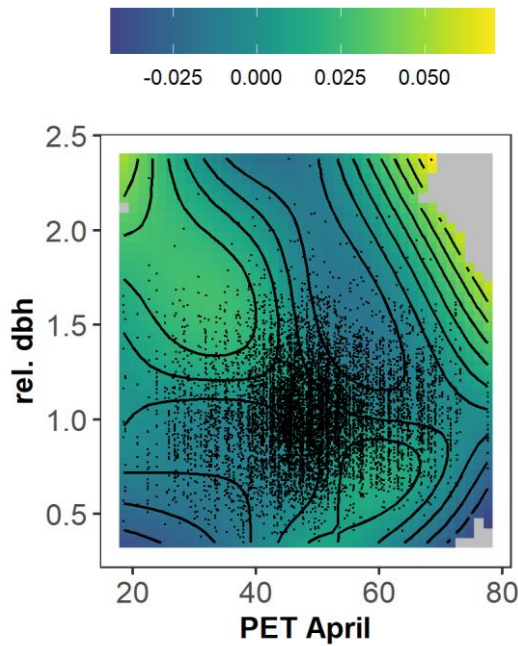
498
499
500
501
502
503

Figure 8: Effect of potential evapotranspiration (PET) in the month of September of the previous year and April–July of the current year on diameter increment for *Pinus sylvestris*. Solid line: prediction, dashed lines confidence interval. Note that the linear predictor ($\ln(\text{diameter increment})$) is zero at the mean of the covariate PET in the respective month.



505
506
507
508
509
510
511
512

Figure 9: Interaction between potential evapotranspiration in the month September of previous year (left) and July from current year (right) for *Quercus robur* and *Quercus petraea* with relative dbh (dbh divided by quadratic mean diameter). Z-values (top of graph) represent the linear predictor ($\ln(\text{diameter increment})$). Dots indicate observed data points. White parts indicate regions with no data points.

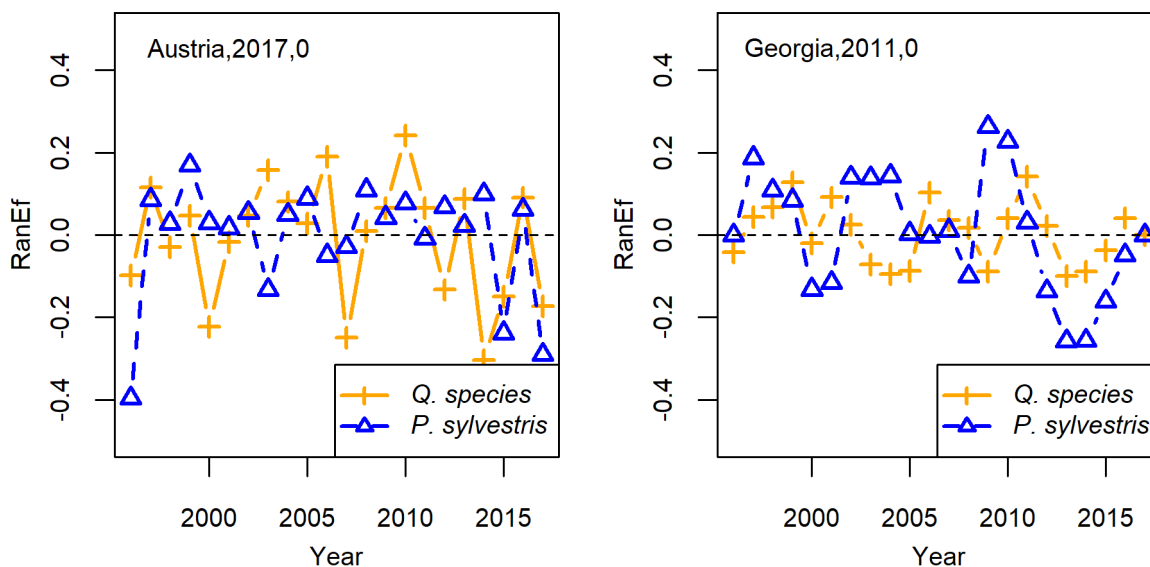


513
514
515
516
517
518
519

Figure 10: Interaction between potential evapotranspiration in the month from April of the current year for *Pinus sylvestris* with relative dbh (dbh divided by quadratic mean diameter). Z-values (top of graph) represent the linear predictor ($\ln(\text{diameter increment})$). Dots indicate observed data points. White parts indicate regions with no data points.

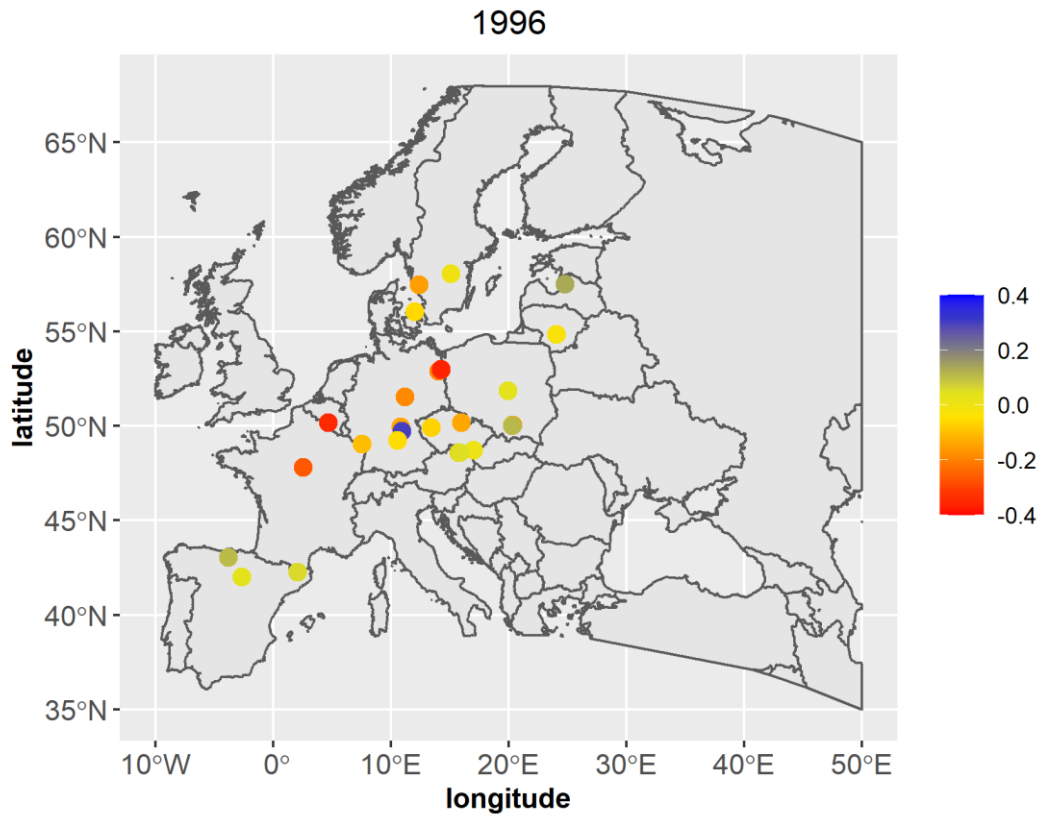
520 3.3 Random effects

521 The temporal trends for both tree species at the same site (Figure 11: two selected
522 plots. Supplementary material 1: all plots) clearly indicate the same growth reaction for both
523 tree genera in some years, but in the years investigated, contrasting patterns prevail at all sites.
524 Similarly, random effects vary between triplets and the triplet effect is year specific (Figure
525 12: two selected years for *Q. spp.*. Supplementary material 2 and 3: all years for both species).
526 The regional site- specific effect is not correlated with the classification in the three broad

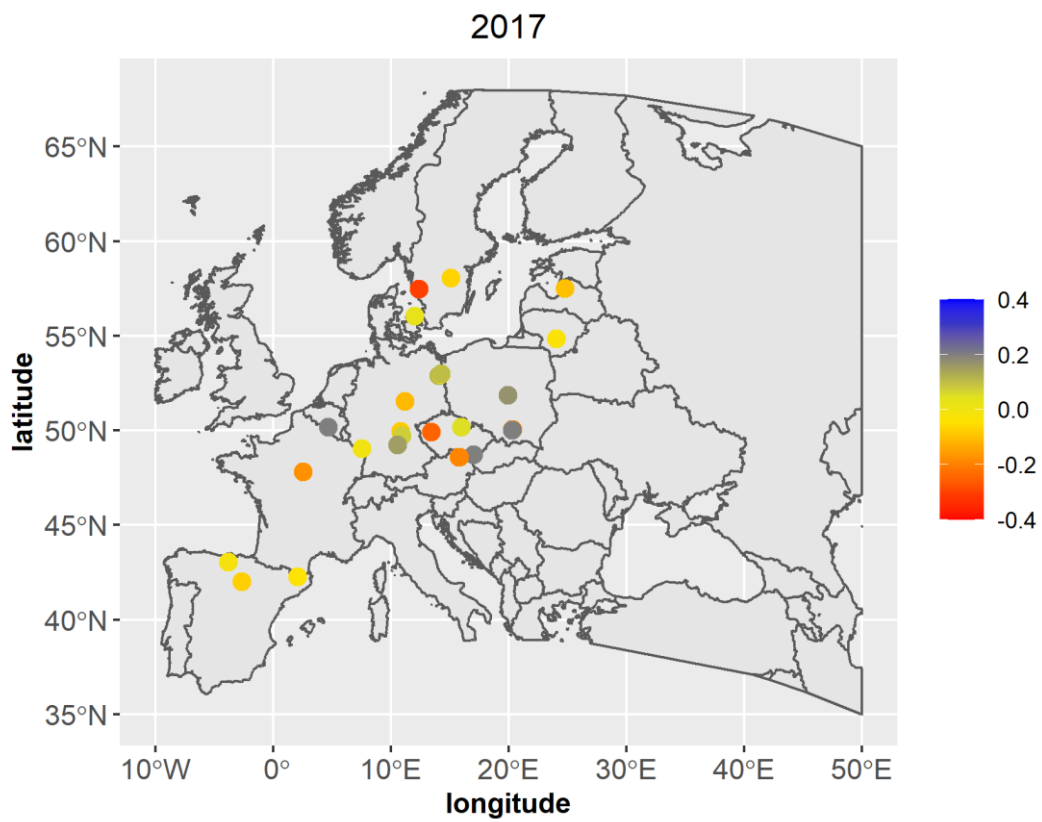


527 climatic classes: Mediterranean climate, temperate climate and boreal climate. Residual
528 diagnostics (Supplementary material 4) indicate an adequate model fit.

529 **Figure 11:** Random temporal trend for two selected plots. Left: Austria, Plot 2017, 0. Right: Georgia, Plot 2011
530 0. RanEf=Random effects ($\ln(\text{diameter increment})$)
531



532



533

534 **Figure 12:** Random triplet effects for *Quercus robur* and *Quercus petraea* for 1996 and 2017. Z-Values represent
 535 the linear predictor ($\ln(\text{diameter increment})$)

536 **4. Discussion**

537 **4.1 Long-term climate and site effects on tree growth**

538 Large-scale spatial patterns drive the occurrence of tree species and the occurrence of
539 specific mixtures or ecotones (Thurm et al. 2018). With climate warming, many tree species
540 will shift their centroids of occurrence and migrate northward (Thurm et al. 2018). Also, tree
541 growth depends on long-term climate (Vospersnik 2021), which was also confirmed in this
542 study. However, only long-term mean temperature was included to represent climatic effects
543 in the best model since the data does not cover all combinations of temperature and
544 precipitation, though covering a large gradient of the single variables. Since not all
545 combinations were covered, long term precipitation was shrunk to the null-space because of
546 concavity with long-term temperature.

547 Other site factors, such as soil type, soil water holding capacity, solar radiation or
548 aspect were represented by the random triplet and plot effects accounting for site-specific
549 growth response. Local soil conditions and local climate between plots within a year are very
550 diverse. The site can be highly contrasting even at small spatial scales (Oberhuber et al.
551 1998).

552 The overall variation explained by the models is 87 %, which is considerably more
553 than 30-70 % reviewed for tree ring studies in an opinion paper by Wilmking et al. (2020).
554 This result indicates that it is important to account for the site and the hierarchical structure of
555 the data by including random effects. Influential factors at the tree level, considered by the
556 random effects, could be tree genetics, management history, or defoliation elicited by insects,
557 which explain a larger proportion of the variation than the site-level random effects.

558 **4.2 Climate during the growing season**

559 Climate during the growing season and tree growth are well correlated, as confirmed
560 by many tree ring studies (Linderholm 2001, Bose et al. 2021, Gillner et al. 2013). The tricky

561 part might be to define the growing season correctly in data sets that span large environmental
562 gradients. Frequently, the period from August of the previous year to September of the current
563 year is considered (Sánchez-Salguero et al. 2013). Surprisingly, significant months found in
564 this study were rather consistent across sites with the influential month being the same on all
565 plots. Tree growth in our study was related to PET in September of the previous year and PET
566 in April-July, whereas PET in late summer and autumn of the current year were not
567 significant. Variables related to ring-width in other tree ring studies were temperature and
568 precipitation (Linderholm and Linderholm 2004, Nothdurft and Engel 2020, Vospernik
569 2021a, Jacobs et al. 2022), PET (Toïgo et al. 2018), vapour pressure deficit (Timofeeva et al.
570 2017, Lindner et al. 2010) or climatic water balance (Árvai et al. 2018) and drought indices
571 (Gomes Marques et al. 2018, Marqués et al. 2021). In our study, PET resulted in the highest
572 R^2 and lowest AIC, but model fit with other climatic variables resulted in a similar model
573 performance except for models including drought indices, with the choice between climate
574 variables being almost arbitrary. Thus, in our study the climate variables themselves are better
575 suited to explain tree growth, then the tested drought indices (De Martonne-index (Martonne
576 1926), SPI (McKee et al. 1993), SPEI (Vicente-Serrano et al. 2010). Models including climate
577 variables have a slightly higher R^2 and lower AIC than models including drought indices. The
578 better overall performance of climate variables may be due to the fact that climate-growth
579 patterns in spring are mainly temperature limited, which in turn might not be well captured by
580 drought indices. The better performance of climate variables is in line with results from
581 temperate sites (Linderholm and Linderholm 2004, Nothdurft and Engel 2020, Vospernik
582 2021a, Toïgo et al. 2018, Timofeeva et al. 2017, Lindner et al. 2010); whereas on
583 Mediterranean sites, drought indices are used in tree ring studies (Gomes Marques et al. 2018,
584 Marqués et al. 2021). We did, however, not detect a dependence of random site effects on the
585 bio-climatic region, and thus think that PET accurately describes tree growth even on
586 Mediterranean sites.

587 *Quercus-Pinus* sites are mostly xeric sites, where water availability is a more
588 important limiting factor for tree growth than temperature (Bose et al. 2021), but the
589 importance of different climatic factors varies throughout the year and is tightly linked to tree
590 ring formation. Tree growth was positively related with higher PET in the spring and early
591 summer month. With sufficient soil moisture from winter rainfall, warm conditions are
592 favourable for tree growth, whereas this pattern switches to a sharp decrease of growth in
593 June with increasing PET. Surprisingly, the climatic influence is again opposite already in
594 July, possibly because of a switch to late-wood production in this month (Rathgeber et al.
595 2016).

596 *Quercus*, as ring-porous species, re-establish their vessels from stored carbohydrates
597 early in spring before leaf-unfolding (Morecroft and Roberts 1999). *P. sylvestris* is
598 anatomically very different and, as conifer species can do photosynthesis during warm periods
599 in winter (Pakharkova et al. 2016). Nevertheless, the beginning of cell formation and tree
600 growth for *P. sylvestris* are also linked to increasing temperatures in spring (e.g. Strieder and
601 Vospernik 2021), with the beginning of tree growth of *P. sylvestris* being sometimes earlier at
602 the same site than for *Q. spp.* (Michelot et al. 2012a), which is confirmed by the significant
603 influence of PET in April for the *P. sylvestris* model and no significant effect of April climate
604 on ring width for *Q. spp.*. With increasing spring temperatures, cell formation and growth
605 rates increase, and maximum growth rates are often observed around the summer solstice (e.g.
606 Strieder and Vospernik 2021). Cell formation takes several weeks (Rathgeber et al. 2016), and
607 for *Q. spp.* there can be a 50-day delay from leaf-unfolding till the trees reach maximum
608 photosynthetic capacity (Morecroft and Roberts 1999). As a consequence, June PET has the
609 most considerable influence on tree growth in our model across all sites. This behaviour is
610 also supported by the fact that spring and early summer droughts are usually crucial for tree
611 growth and better correlated with ring width (Bose et al. 2021, Gillner et al. 2013) than
612 summer or autumn droughts. Subsequently, in July, trees switch from early-wood formation

613 to late-wood formation, and the production of new cells ceases in time before winter to
614 protect the sensitive cambium from frost (Rathgeber et al. 2016). Photosynthetic products
615 from autumn are stored and affect next years' tree ring formation in *Quercus*, but less so for
616 *P. sylvestris* (Michelot et al. 2012b). In line with this physiological behaviour, tree ring width
617 for both tree genera (*Quercus*, *Pinus*) is influenced by September PET, but patterns are more
618 evident for *Q. spp.*. Such correlations with last years' temperature are likewise reported in
619 other studies (*Quercus* (e.g. Gillner et al. 2013); *Pinus* (e.g. Sánchez-Salguero et al. 2013)).
620 Similarly, to the lagged influence of autumn climate, growth reductions due to drought are
621 also observed in the following years (Bose et al. 2021, Gillner et al. 2013), but the long-term
622 impact of drought must be considered marginal for *Quercus spp.* (Gillner et al. 2013) since
623 post-drought effects for *Quercus spp.* are observed for 1-2 years (Gillner et al. 2013, Vitasse
624 et al. 2019). In contrast, growth of conifers is enduringly reduced by spring drought (Vitasse
625 et al. 2019) and recovery from drought spells for *P. sylvestris* is reported to be slower (more >
626 5 years) (Galiano et al. 2011) than for *Quercus*. Moreover, results by Bose et al. 2020 indicate
627 that *P. sylvestris* trees that experienced more frequent droughts (e.g. series of drought years
628 like 2015, 2018, 2019 in Europe) over the long-term are less resistant to extreme droughts.
629 Thus, more frequent and longer predicted drought periods in the future may overstrain *P.*
630 *sylvestris* potential for acclimation. This, however, could be buffered to some extent by
631 favoring *Quercus-Pinus* mixed forest stands over monocultures of both tree species on
632 mesotrophic xeric and mesic sites (Steckel et al. 2020a).

633 **4.3 Age, competition and social position**

634 Tree growth declined with age; this age trend was modelled for the whole population
635 and tree ring series specific. Modelling or removing the age trend is key in studying the
636 climate-growth relationship and is the standard in tree ring research (e.g. Linderholm 2001,
637 Bose et al. 2021, Gillner et al. 2013, Schmitt et al. 2020). In this study, we opted for
638 modelling the age trend, since we were interested in the trend itself. The age trend was

639 consistent, showing a steady decline with age. This is because the stands investigated are all at
640 an age past the maximum of individual tree diameter increment. Similarly, we included other
641 factors such as competition and social position, which are treated as noise in tree ring studies
642 and a smooth from tree ring series using splines. From the various competition indices tested,
643 local SDI was included in the final model. This index resulted in the highest R^2 and lowest
644 AIC, although differences were almost identical (<0.01 difference in R^2) compared to
645 potential models including different competition indices. The major advantage of local SDI is
646 that it showed consistent patterns in many model formulations, indicating little concurrency
647 with other variables. In particular, its independence of age facilitates the development of
648 multivariate models (e.g. Burkhart and Tomé 2012). The relationship found for studied tree
649 species is quite similar in both magnitude and form, with a stronger decrease for *P. sylvestris*
650 at higher densities. We refrained from including dbh in the model since tree size increases
651 with both age and social position making it difficult to separate the respective effects. Social
652 position is known to significantly affect growth duration, with suppressed trees having a
653 shorter period of growth than dominant ones (e.g. Rathgeber et al. 2011, Strieder and
654 Vospernik 2021). Interactions between social position and climate found in this study might
655 reflect this different behavior observed in studies on intra-annual growth.

656 **4.4 Mixture and stand structure**

657 Positive mixture effects on productivity at the stand level were reported for the
658 *Quercus-Pinus* triplet gradient (Pretzsch et al. 2020, Steckel et al. 2020a, del Rio et al. 2022).
659 At the individual tree level, positive mixture effects are also observed, but are only significant
660 for *P. sylvestris*, once the overall model accounts for stand density and structure. Beneficial
661 mixture effects at the individual tree level result from higher nutrient availability (Thelin et al.
662 2002, Aubert et al. 2006, Nickmans et al. 2015), hydraulic lift (Muñoz-Gálvez et al. 2021) and
663 complementary light use efficiency because of different crown structure and leave phenology
664 (Kelty et al. 1992, Pretzsch and Schütze 2016, Ammer 2019) all of which seem to affect *Pinus*

665 mainly positively. This behavior is in line with the ecophysiology of the two genera since *Q.*
666 *spp.* has the more nutrient-rich leaves (Yuste et al. 2005) and a deeper rooting system.
667 Differences in stand density between species and differences in stand structure may be
668 important reasons why the effects of mixture on productivity differ between stand and
669 individual tree levels (Pretzsch and Schütze 2016). For the species investigated here, *P.*
670 *sylvestris* has a considerably higher maximum density than *Q. spp.* (Vospernik and Sterba
671 2015) and this higher potential density of *P. sylvestris* may be an important reason for
672 differing results at the stand level and the individual tree levels, because it indicates different
673 use of space of the two species. The temporal patterns of the random effects show that trees'
674 species-specific effects can strongly vary between tree species at the same site and for
675 particular years. Other studies also reported varying between-year effects (Strieder and
676 Vospernik 2021). Given the 20-years analyzed in this study, the population results reported
677 characterize tree species behavior, but also show that caution needs to be exercised when
678 analyzing shorter periods since effects strongly fluctuate. There was no consistent interaction
679 effect between climate and mixture. Thus, the mitigating effect of mixture on growth for the
680 species investigated could not be shown.

681 **5. Conclusions**

682 The relationship between tree growth and climate change is an important
683 contemporary question at large spatial scales. Inference from single case studies is complex.
684 and pooling Europe-wide data or data from different sources is needed to enhance
685 understanding of the climate growth relationship and facilitate growth prognosis at larger
686 scales. This study shows that tree ring data can be modelled over large environmental
687 gradients by accounting for random tree and site effects, explaining 87 % of the total
688 variation. This correct statistical specification results in climate – growth relationships that are
689 well in line with our current physiological understanding from more detailed dendrometer

690 studies. Climate reactions across Europe have a standard population signal, and the most
691 significant influence of climate on tree growth is in June, at the maximum day length, but the
692 direction and magnitude of climatic effects vary throughout the growing seasons. This varying
693 strength and direction of seasonal climatic effects are rarely accounted for in modelling tree
694 growth response, where the average climate for the whole growing season is often included.
695 In future studies, accounting for a monthly or daily climate in forest growth models should
696 receive more emphasis.

697 An interesting finding is the high temporal dynamic at the same site, emphasizing the
698 importance of considering several years in tree growth analysis. Tree species mixture has a
699 positive effect on productivity. However, this effect is small compared to the climatic
700 impacts. Thus, the mixture may only partly mitigate growth reductions due to drought. Rather
701 large effects on diameter increment are observed due to stand structure but cannot be
702 systematically explained in this study or related to silvicultural management.

703 Growth factors are manifold and interrelated, and tree ring models are thus prone to
704 concurvity. Nevertheless, we advocate an overall model approach, which in contrast to
705 dendrochronological studies, allows testing other growth factors and interactions thereof with
706 climate. Concurvity can be well avoided by including variables that are considered free of the
707 influence of other growth factors.

708

709 **Acknowledgements**

710 The authors thank the European Union for funding the project "Mixed species forest
711 management. Lowering risk, increasing resilience (REFORM)" under the framework of
712 Sumforest ERA-NET. All contributors thank their national funding institutions to establish,
713 measure and analyze data from the triplets. The Polish State Forests Enterprise also supported
714 one of the Polish co-authors (Grant No: OR.271.3.15.2017). The Orléans site, OPTMix was

715 installed thanks to ONF (National Forest Service, France), belongs to research infrastructure
716 ANAEE-F; it is also included in the SOERE TEMPO, ZAL (LTSER Zone Atelier Loire) and
717 the GIS oop network. This work was also supported by grant APVV-18-0347 (Slovakia). We
718 acknowledge Institutional support MZE-RO0118 from the Ministry of Agriculture of the
719 Czech Republic, partly funding the field measurements at Czech triplets.

720 **References**

- 721 Akaike, H. 1973. Information theory as an extension of the maximum likelihood principle. *In*
722 Second international symposium on information theory Akademiai. *Edited by* B.N.
723 Petrov and F. Csaksi. Kiado Budapest. pp. 267–281.
- 724 Ammer, C. 2019. Diversity and forest productivity in a changing climate. *New Phytol* **221**:
725 50–66. doi:10.1111/nph.15263
- 726 Arend, M., Kuster, T., Günthardt-Goerg, M.S., and Dobbertin, M. 2011. Provenance-specific
727 growth responses to drought and air warming in three European oak species (*Quercus*
728 *robur*, *Q. petraea* and *Q. pubescens*). *Tree Physiol.* 31(3)287-297. doi:10.1093/tr **31**(3):
729 287–297. doi:10.1093/treephys/tpr004.
- 730 Árvai, M., Morgós, A., and Kern, Z. 2018. Growth-climate relations and the enhancement of
731 drought signals in pedunculate oak (*Quercus robur* L.) tree-ring chronology in Eastern
732 Hungary. *IForest* **11**(2): 267–274. doi:10.3832/ifor2348-011.
- 733 Aubert, M., Margerie, P., Ernoult, A., Decaëns, T., and Bureau, F. 2006. Variability and
734 heterogeneity of humus forms at stand level: Comparison between pure beech and mixed
735 beech-hornbeam forest. *Ann. For. Sci.* **63**: 177–188. doi: 10.1051/forest:2005110
- 736 Barsoum, N., Eaton, E.L., Levanič, T., Pargade, J., Bonnart, X., and Morison, J.I.L. 2015.
737 Climatic drivers of oak growth over the past one hundred years in mixed and
738 monoculture stands in southern England and northern France. doi:10.1007/s10342-014-
739 0831-5.
- 740 Bhuyan, U., Zang, C., and Menzel, A., 2017. Different Responses of Multispecies Tree Ring
741 Growth to Various Drought Indices Across Europe. *Dendrochronologia* **44** (6): 1–8. doi:
742 10.1016/j.dendro.2017.02.002.
- 743 Biging, G., and Dobbertin, M. 1992. A comparison of distance-dependent competition
744 measures for height and basal area growth of individual conifer trees. *For. Sci.* **38**(3):
745 695–720.
- 746 Biging, G.S., and Dobbertin, M. 1995. Evaluation of competition indices in individual tree
747 growth models. *For. Sci.* **41**(2): 360–377.
- 748 Bigler, C., Bräker, O.U., Bugmann, H., Dobbertin, M., and Rigling, A. 2006. Drought as an
749 inciting mortality factor in scots pine stands of the Valais, Switzerland. *Ecosystems* **9**(3):
750 330–343. doi:10.1007/s10021-005-0126-2.
- 751 Binkley, D., Kashian, D.M., Boyden, S., Kaye, M.W., Bradford, J.B., Arthur, M.A., Fornwalt,
752 P.A., Ryan, M.G. 2006. Patterns of growth dominance in forests of the Rocky

- 753 Mountains. USA For. Ecol. Manage. **236**: 193-201
- 754 Bose, A.K., Scherrer, D., Camarero, J.J., Ziche, D., Babst, F., Bigler, C., Bolte, A., Dorado-
755 Liñán, I., Etzold, S., Fonti, P., Forrester, D.I., Gavinet, J., Gazol, A., de Andrés, E.G.,
756 Karger, D.N., Lebourgeois, F., Lévesque, M., Martínez-Sancho, E., Menzel, A.,
757 Neuwirth, B., Nicolas, M., Sanders, T.G.M., Scharnweber, T., Schröder, J., Zweifel, R.,
758 Gessler, A., and Rigling, A. 2021. Climate sensitivity and drought seasonality determine
759 post-drought growth recovery of *Quercus petraea* and *Quercus robur* in Europe. Sci.
760 Total Environ. **784**: 147222. doi:10.1016/j.scitotenv.2021.147222.
- 761 Bose, A.K., Gessler, A., Bolte, A., Bottero, A., Buras, A., Cailleret, M., Camarero, J.J., Haeni,
762 M., Hereş, A.M., Hevia, A., Lévesque, M., Linares, J.C., Martínez-Vilalta, J., Matías, L.,
763 Menzel, A., Sánchez-Salguero, R., Saurer, M., Vennetier, M., Ziche, D., Rigling, A.,
764 2020. Growth and resilience responses of Scots pine to extreme droughts across Europe
765 depend on predrought growth conditions. Glob. Chang. Biol. **26**: 4521–4537.
766 <https://doi.org/10.1111/gcb.15153>
- 767 Burkhardt, H.E., and Tomé, M., 2012. Modeling Forest Trees and Stands. Springer Netherlands.
768 Dordrecht. doi:10.1007/978-90-481-3170-9.
- 769 Collet, C., Manso, R., and Barbeito, I. 2017. Coexistence, association and competitive ability
770 of *Quercus petraea* and *Quercus robur* seedlings in naturally regenerated mixed stands.
771 For. Ecol. Manage. **390**: 36–46. doi:10.1016/j.foreco.2017.01.021.
- 772 Del Río, M., Pretzsch, H., Ruiz-Peinado, R., Jactel, H., Coll, L., Löf, M., Aldea, J., Ammer,
773 C., Avdagić, A., Barbeito, I., Bielak, K., Bravo, F., Brazaitis, G., Cerný, J., Collet, C.,
774 Condés, S., Drössler, L., Fabrika, M., Heym, M., Holm, S.-O., Hysten, G., Janson, A.,
775 Kurylak, V., Lombardi, F., Matović, B., Metslaid, M., Motta, R., Nord-Larsen, T.,
776 Nothdurft, A., den Ouden, J., Pach, M., Pardos, M., Poeydebat, C., Ponette, Q., Pérot, T.,
777 Reventlow, D., Sitko, R., Sramek, V., Steckel, M., Svoboda, M., Verheyen, K.,
778 Vospernik, S., Wolff, B., Zlatanov, T., Bravo-Oviedo, A., 2022. Emerging Stability of
779 Forest Productivity by Mixing Two Species Buffers Temperature Destabilizing Effect.
780 Journal of Applied Ecology. 59(11): 2730-2741. doi: 10.1111/1365-2664.14267.
- 781 Dirnberger, G., Sterba, H., Condés, S., Ammer, C., Annighöfer, P., Avdagić, A., Bielak, K.,
782 Brazaitis, G., Coll, L., Heym, M., Hurt, V., Kurylyak, V., Motta, R., Pach, M., Ponette,
783 Q., Ruiz-Peinado, R., Skrzyszewski, J., Šrámek, V., de Streel, G., Svoboda, M.,
784 Zlatanov, T., and Pretzsch, H. 2017. Species proportions by area in mixtures of Scots
785 pine (*Pinus sylvestris* L.) and European beech (*Fagus sylvatica* L.). Eur. J. For. Res.
786 **136**(1): 171–183. doi:10.1007/s10342-016-1017-0.
- 787 Durrant, T.H., de Rigo, D., and Caudullo, G. 2016. *Pinus sylvestris* in Europe: distribution,
788 habitat usage and threats. In: San-Miguel-Ayanz, J., de Rigo, D., Caudullo, G., Houston
789 Durrant, T., Mauri, A. (Eds.). European Atlas of Forest Tree Species. Publ. Off. EU.
790 Luxembourg. pp. e016b94++
- 791 Eaton, E., Caudullo, G., Oliveira, S., and de Rigo, D. 2016. *Quercus robur* and *Quercus*
792 *petraea* in Europe: distribution, habitat, usage and threats. In: San-Miguel-Ayanz, J., de
793 Rigo, D., Caudullo, G., Houston Durrant, T., Mauri, A. (Eds.). European Atlas of Forest
794 Tree Species. Publ. Off. EU. Luxembourg. pp. e01c6df+
- 795 Eilmann, B., Weber, P., Rigling, A., and Eckstein, D. 2006. Growth reactions of *Pinus*
796 *syvestris* L. and *Quercus pubescens* Willd. to drought years at a xeric site in Valais,
797 Switzerland. Dendrochronologia **23**(3): 121–132. doi:10.1016/j.dendro.2005.10.002.

- 798 Epron D., and Dreyer, E. 1993. Long- term effects of drought on photosynthesis of adult oak
799 trees [*Quercus petraea* (Matt.) Liebl. and *Quercus robur* L.] in a natural stand. New
800 Phytol. **125**(2): 381–389. doi:10.1111/j.1469-8137.1993.tb03890.x.
- 801 Feichtinger, L.M., Eilmann, B., Buchmann, N., and Rigling, A. 2014. Growth adjustments of
802 conifers to drought and to century-long irrigation. For. Ecol. Manage. **334**: 96–105.
803 doi:10.1016/j.foreco.2014.08.008.
- 804 Forrester, D.I. 2014. The Spatial and Temporal Dynamics of Species Interactions in Mixed-
805 Species Forests: From Pattern to Process. For. Ecol. Manage. **312**: 282-292 doi:
806 10.1016/j.foreco.2013.10.003.
- 807 Galiano, L., Martínez-Vilalta, J., and Lloret, F. 2011. Carbon reserves and canopy defoliation
808 determine the recovery of Scots pine 4yr after a drought episode. New Phytol. **190**(3):
809 750–759. doi:10.1111/j.1469-8137.2010.03628.x.
- 810 Gillner, S., Vogt, J., and Roloff, A. 2013. Climatic response and impacts of drought on oaks
811 at urban and forest sites. Urban For. Urban Green. **12**(4): 597–605.
812 doi:10.1016/j.ufug.2013.05.003.
- 813 Gomes Marques, I., Campelo, F., Rivaes, R., Albuquerque, A., Ferreira, M.T., and Rodríguez-
814 González, P.M. 2018. Tree rings reveal long-term changes in growth resilience in
815 Southern European riparian forests. Dendrochronologia **52**: 167–176.
816 doi:10.1016/j.dendro.2018.10.009.
- 817 Harris, I., Osborn, T.J., Jones, P., and Lister, D. 2020. Version 4 of the CRU TS monthly
818 high-resolution gridded multivariate climate dataset. Sci. Data **7**(1): 1–18.
819 doi:10.1038/s41597-020-0453-3.
- 820 Hastie, T.J., and Tabshirani, R.J. 1990. Generalized Additive Models. New York.
- 821 Hegyi, F. 1974. A simulation model for managing jack-pine stands. *In*: Growth models for
822 tree and stand simulation. Edited by J. Fries: 74–90.
- 823 Höwler, K., Vor, T., Seidel, D., Annighöfer, P., Ammer, Ch. 2019. Analyzing Effects of
824 Intra- and Interspecific Competition on Timber Quality Attributes of *Fagus Sylvatica*
825 L.—from Quality Assessments on Standing Trees to Sawn Boards. Eur. J. For. Res. **138**:
826 327-343. doi:10.1007/s10342-019-01173-7
- 827 Jacobs, K., Jonard, M., Muys, B., Ponette, Q. 2022. Shifts in dominance and complementarity
828 between sessile oak and beech along ecological gradients. Journal of Ecology. **110**:
829 2404-2417. doi: 10.1111/1365-2745.13958
- 830 Kelty, M.J., Larson, B.C., Oliver, C.D. 1992. The ecology and silviculture of mixed-species
831 forests: a festschrift for David M. Smith. Springer Netherlands. Dordrecht. doi:
832 10.1007/978- 94-015-8052-6
- 833 Leuzinger, S., Zotz, G., Asshoff, R., and Körner, C. 2005. Responses of deciduous forest trees
834 to severe drought in Central Europe. Tree Physiol. **25**(6): 641–650.
835 doi:10.1093/treephys/25.6.641.
- 836 Linderholm, H.W., 2001. Climatic influence on scots pine growth on dry and wet soils in the
837 central Scandinavian mountains. interpreted from tree-ring widths. Silva Fenn. **35**(4):
838 415–424. doi:10.14214/sf.574.

- 839 Linderholm, H.W., and Linderholm, K. 2004. Age-dependent climate sensitivity of *Pinus*
840 *sylvestris* L. in the central Scandinavian Mountains. *Boreal Environ. Res.* **9**(4): 307–317.
- 841 Lindner, M., Maroschek, M., Netherer, S., Kremer, A., Barbati, A., Garcia-Gonzalo, J., Seidl,
842 R., Delzon, S., Corona, P., Kolström, M., Lexer, M.J., and Marchetti, M. 2010. Climate
843 change impacts, adaptive capacity, and vulnerability of European forest ecosystems. *For.*
844 *Ecol. Manage.* **259**(4): 698–709. doi:10.1016/j.foreco.2009.09.023.
- 845 Marqués, L., Camarero, J.J., Zavala, M.A., Stoffel, M., Ballesteros-Cánovas, J.A., Sancho-
846 García, C., and Madrigal-González, J. 2021. Evaluating tree-to-tree competition during
847 stand development in a relict Scots pine forest: how much does climate matter? *Trees -*
848 *Struct. Funct.* **35**(4): 1207–1219. doi:10.1007/s00468-021-02109-8.
- 849 Marra, G., Wood, S.N. 2011. Practical Variable Selection for Generalized Additive Models
850 *Computational Statistics & Data Analysis* **55** (7): 2372–87. doi:
851 10.1016/j.csda.2011.02.004.
- 852 Martín-Gómez, P., Aguilera, M., Pemán, J., Gil-Pelegrián, E., and Ferrio, J.P. 2017.
853 Contrasting ecophysiological strategies related to drought: the case of a mixed stand of
854 Scots pine (*Pinus sylvestris*) and a submediterranean oak (*Quercus subpyrenaica*). *Tree*
855 *Physiol.* **37**(11): 1478–1492. doi:10.1093/treephys/tpx101.
- 856 Martonne, D. 1926. Une nouvelle fonction climatologique: L'indice d'aridité. *La Météorologie*
857 **21**: 449–458.
- 858 McKee, T.B., Doesken, N.J., and Kleist, J. 1993. The relationship of drought frequency and
859 duration to time scales. *In* Proceedings of the Eighth Conference on Applied
860 Climatology. 17–22 January 1993 Boston. American Meteorological Society. Anaheim.
861 California. Pp. 179-184.
- 862 Mellert, K.H., Göttlein, A., 2012. Comparison of new foliar nutrient threshold derived from
863 van den Burg's literature compilation with established central European references. *Eur.*
864 *J. For. Res.* **131**: 1461-1472. doi: 10.1007/s10342-012-0615-8
- 865 Mérian, P., Pierrat, J.C., and Lebourgeois, F. 2013. Effect of sampling effort on the regional
866 chronology statistics and climate-growth relationships estimation. *Dendrochronologia*
867 **31**(1): 58–67. doi:10.1016/j.dendro.2012.07.001.
- 868 Merlin, M., Perot, T., Perret, S., Korboulewsky, N., Vallet, P., 2015. Effects of stand
869 composition and tree size on resistance and resilience to drought in sessile oak and Scots
870 pine. *For. Ecol. Manage.* **339** 22-33. doi: 10.1016/j.foreco.2014.11.032
- 871 Michelot, A., Bréda, N., Damesin, C., and Dufrêne, E. 2012a. Differing growth responses to
872 climatic variations and soil water deficits of *Fagus sylvatica*, *Quercus petraea* and *Pinus*
873 *sylvestris* in a temperate forest. *For. Ecol. Manage.* **265**: 161–171.
874 doi:10.1016/j.foreco.2011.10.024.
- 875 Michelot, A., Simard, S., Rathgeber, C., Dufrêne, E., and Damesin, C. 2012b. Comparing the
876 intra-annual wood formation of three European species (*Fagus sylvatica*, *Quercus*
877 *petraea* and *Pinus sylvestris*) as related to leaf phenology and non-structural
878 carbohydrate dynamics. *Tree Physiol.* **32**(8): 1033–1045. doi:10.1093/treephys/tps052.
- 879 Morecroft, M.D., and Roberts, J.M. 1999. Photosynthesis and stomatal conductance of mature
880 canopy Oak (*Quercus robur*) and Sycamore (*Acer pseudoplatanus*) trees throughout the
881 growing season. *Funct. Ecol.* **13**(3): 332–342. doi:10.1046/j.1365-2435.1999.00327.x.

- 882 Muller, S. 1992. Natural acidophilous *Quercus* and *Pinus* forests in the northern Vosges,
883 France, from a geographical perspective. *J. Veg. Sci.* **3**(5): 631–636.
884 doi:10.2307/3235830.
- 885 Muñoz-Gálvez, F.J., Herrero, A., Esther Pérez-Corona, M., and Andivia, E. 2021. Are pine-
886 oak mixed stands in Mediterranean mountains more resilient to drought than their
887 monospecific counterparts? *For. Ecol. Manage.* **484**: 118955
888 doi:10.1016/j.foreco.2021.118955.
- 889 Nickmans, H., Verheyen, K., Guiz, J., Jonard, M., Ponette, Q. 2015. Effects of neighbourhood
890 identity and diversity on the foliar nutrition of sessile oak and beech. *For. Ecol. Manage.*
891 **335**: 108–117. doi: 10.1016/j.foreco.2014.09.025
- 892 Nothdurft, A., and Engel, M. 2020. Climate sensitivity and resistance under pure- and mixed-
893 stand scenarios in Lower Austria evaluated with distributed lag models and penalized
894 regression splines for tree-ring time series. *Eur. J. For. Res.* **139**(2): 189–211.
895 doi:10.1007/s10342-019-01234-x.
- 896 Oberhuber, W., Stumböck, M., Kofler, W. 1998. Climate-tree-growth relationships of Scots
897 pine stands (*Pinus sylvestris* L.) exposed to soil dryness. *Trees* **13**: 19–27 doi:
898 10.1007/PL00009734.
- 899 Pakharkova, N. V., Heilmeyer, H., Gette, I.G., Andreeva, E.B., Grachev, A.M., Gaevskiy,
900 N.A., and Grigoriev, Y.S. 2016. Quantitative characteristics of the phases of winter
901 dormancy of conifer species at a site in Central Siberia. *Rev. Bras. Bot.* **39**(4): 1005–
902 1014. doi:10.1007/s40415-016-0298-3.
- 903 Pommerening, A., and Stoyan, D. 2006. Edge-correction needs in estimating indices of spatial
904 forest structure. *Can. J. For. Res.* **36**(7): 1723–1739. doi:10.1139/X06-060.
- 905 Pretzsch, H. 2009. *Forest Dynamics. Growth and Yield.* Springer Verlag.
- 906 Pretzsch, H., and Biber, P. 2010. Size-symmetric versus size-asymmetric competition and
907 growth partitioning among trees in forest stands along an ecological gradient in central
908 Europe. *Can. J. For. Res.* **40**(2): 370–384. doi:10.1139/X09-195.
- 909 Pretzsch, H., and Biber, P. 2016. Tree species mixing can increase maximum stand density.
910 *Can. J. For. Res.* **46**(10): 1179–1193. doi:10.1139/cjfr-2015-0413.
- 911 Pretzsch, H., Forrester, D.I., and Bauhus, J. 2017. *Mixed-species forests: ecology and
912 management.* Springer. Heidelberg.
- 913 Pretzsch, H., and Del Río, M. 2020. Density regulation of mixed and mono-specific forest
914 stands as a continuum: A new concept based on species-specific coefficients for density
915 equivalence and density modification. *Forestry* **93**(1): 1–15.
916 doi:10.1093/forestry/cpz069.
- 917 Pretzsch, H., and Schütze, G. 2016. Effect of tree species mixing on the size structure,
918 density, and yield of forest stands. *Eur. J. For. Res.* **135**(1): 1–22. doi:10.1007/s10342-
919 015-0913-z.
- 920 Pretzsch, H., Steckel, M., Heym, M., Biber, P., Ammer, C., Ehbrecht, M., Bielak, K., Bravo,
921 F., Ordóñez, C., Collet, C., Vast, F., Drössler, L., Brazaitis, G., Godvod, K., Jansons, A.,
922 de-Dios-García, J., Löf, M., Aldea, J., Korboulewsky, N., Reventlow, D.O.J., Nothdurft,
923 A., Engel, M., Pach, M., Skrzyszewski, J., Pardos, M., Ponette, Q., Sitko, R., Fabrika,

- 924 M., Svoboda, M., Černý, J., Wolff, B., Ruíz-Peinado, R., and del Río, M. 2020. Stand
925 growth and structure of mixed-species and monospecific stands of Scots pine (*Pinus*
926 *sylvestris* L.) and oak (*Q. robur* L., *Quercus petraea* (Matt.) Liebl.) analysed along a
927 productivity gradient through Europe. *Eur. J. For. Res.* **139**(3): 349–367.
928 doi:10.1007/s10342-019-01233-y.
- 929 Prodan, M. 1968a. Einzelbaum. Stichprobe und Versuchsfläche. *Allg. Forst- und Jagdzeitung*
930 **139**(10): 239–248.
- 931 Prodan, M. 1968b. Zur Gesetzmäßigkeit der Flächenverteilung von Bäumen. *Allg. Forst- und*
932 *Jagdzeitung* **139**.
- 933 Radtke, P.J., and Burkhardt, H.E. 1998. A comparison of methods for edge-bias compensation.
934 *Can. J. For. Res.* **28**(6): 942–945. doi:10.1139/x98-062.
- 935 Ramírez-Valiente, J.A., López, R., Hipp, A.L., and Aranda, I. 2020. Correlated evolution of
936 morphology, gas exchange, growth rates and hydraulics as a response to precipitation
937 and temperature regimes in oaks (*Quercus*). *New Phytol.* **227**(3): 794–809.
938 doi:10.1111/nph.16320.
- 939 Rathgeber, C.B.K., Rossi, S., Bontemps J.-D. 2011. Cambial activity related to tree size in a
940 mature silver-fir plantation. *Ann Bot-London* **108**: 429–438.
941 <https://doi.org/10.1093/aob/mcr168>
- 942 Rathgeber, C.B.K., Cuny, H.E., and Fonti, P. 2016. Biological basis of tree-ring formation: A
943 crash course. *Front. Plant Sci.* **7**: 1–7. doi:10.3389/fpls.2016.00734.
- 944 Reineke, L.H. 1933. Perfecting a stand-density index for even-aged forests. *J. Agric. Res.* **46**:
945 627–638.
- 946 Rigling, A., Waldner, P.O., Forster, T., and Bräker, O.U. 2001. Ecological interpretation of
947 tree-ring width and intraannual density fluctuations in *Pinus sylvestris* on dry sites in the
948 central Alps and Siberia. **31**: 18–31.
- 949 Rogers, B.M., Solvik, K., Hogg, E.H., Ju, J., Masek, J.G., Michaelian, M., Berner, L.T., and
950 Goetz, S.J. 2018. Detecting early warning signals of tree mortality in boreal North
951 America using multiscale satellite data. *Glob. Chang. Biol.* **24**(6): 2284–2304.
952 doi:10.1111/gcb.14107.
- 953 Roloff, A., Bärtels, A. 2006. *Flora der Gehölze*. Stuttgart: Ulmer
- 954 Salomón, R. L., Peters, R. L., Zweifel, R., Sass-Klaassen, U. G., Stegehuis, A. I., Smiljanic,
955 M., Poyatos, R., Babst, F., Cienciala, E., Fonti, P., Lerink, B. JW., Lindner, M.,
956 Martinez-Vilalta, J., Mencuccini, M., Nabuurs, G.-J., van der Maaten, E., von Arx G.,
957 Bär, A., Akhmetzyanov, L., Balanzategui, D., Bellan, M., Bendix, J., Berveiller, D.,
958 Blaženec, M., Čada, V., Carraro, V., Cecchini, S., Chan, T., Conedera, M., Delpierre, N.,
959 Delzon, S., Ditmarová, L., Dolezal, J., Dufrêne, E., Edvardsson J., Ehekircher, S.,
960 Forner, A., Frouz, J., Ganthaler, A., Gryc, V., Güney, A., Heinrich, I., Hentschel, R.,
961 Janda, P., Ježík, M., Kahle, H.-P., Knüsel, S., Krejza, J. Ľ., Kuberski, Ľ., Kučera, J.,
962 Lebourgeois, F., Mikoláš, M., Matula, R., Mayr, S., Oberhuber, W., Obojes, N.,
963 Osborne, B., Paljakka, T., Plichta, R., Rabbal, I., Rathgeber, C.B.K, Salmon, Y.,
964 Saunders, M., Scharnweber, T., Sitková, Z., Stangler, D. F., Stereńczak, K., Stojanović,
965 M., Střelcová, K., Světlík, J., Svoboda, M., Tobin, B., Trotsiuk, V., Urban, J.,
966 Valladares, F., Vavrčík, H., Vejpustková, M., Walthert L., Wilmking, M., Zin, E., Zou, J.

- 967 & Steppe, K. (2022). The 2018 European heatwave led to stem dehydration but not to
968 consistent growth reductions in forests. *Nature communications*. **13**(1): 1-11.
- 969 Sánchez-Salguero, R., Camarero, J.J., Dobbertin, M., Fernández-Cancio, Á., Vilà-Cabrera, A.,
970 Manzanedo, R.D., Zavala, M.A., and Navarro-Cerrillo. R.M. 2013. Contrasting
971 vulnerability and resilience to drought-induced decline of densely planted vs. natural
972 rear-edge *Pinus nigra* forests. *For. Ecol. Manage.* **310**: 956–967.
973 doi:10.1016/j.foreco.2013.09.050.
- 974 Schweingruber, F.H., Eckstein, D., Serre-Bachet, F., and Bräker, O.U. 1990. Identification.
975 presentation and interpretation of event years and pointer years in dendrochronology.
976 *Dendrochronologia* **9**: 9–38.
- 977 Speer, J.H. 2010. *Fundamentals of tree-ring research*. University of Arizona Press.
- 978 Steckel, M., Heym, M., Wolff, B., Reventlow, D.O.J., Pretzsch, H. 2019. Transgressive
979 overyielding in mixed compared with monospecific Scots pine (*Pinus sylvestris* L.) and
980 oak (*Quercus robur* L., *Quercus petraea* (Matt.) Liebl.) stands – Productivity gains
981 increase with annual water supply. *For. Ecol. Manage.* **439**: 81-96. doi:
982 10.1016/j.foreco.2019.02.038.
- 983 Steckel, M., del Río, M., Heym, M., Aldea, J., Bielak, K., Brazaitis, G., Černý, J., Coll, L.,
984 Collet, C., Ehbrecht, M., Jansons, A., Nothdurft, A., Pach, M., Pardos, M., Ponette, Q.
985 Reventlow, D.O.J., Sitko, R., Svoboda, M., Vallet, P., Wolff, B., and Pretzsch H. 2020a.
986 Species mixing reduces drought susceptibility of Scots pine (*Pinus sylvestris* L.) and oak
987 (*Quercus robur* L., *Quercus petraea* (Matt.) Liebl.) – Site water supply and fertility
988 modify the mixing effect. *For. Ecol. Manage.* **461**: 117908.
989 doi:10.1016/j.foreco.2020.117908.
- 990 Steckel, M., Moser, W.K., del Río, M., Pretzsch, H. 2020b. Implications of Reduced Stand
991 Density on Tree Growth and Drought Susceptibility: A Study of Three Species under
992 Varying Climate. *Forests*. **11**(6): 627. doi:10.3390/f11060627.
- 993 Strieder, E., and Vospernik, S. 2021. Intra-annual diameter growth variation of six common
994 European tree species in pure and mixed stands. *Silva Fenn.* **55**(4): 10449.
995 doi:10.14214/sf.10449.
- 996 Suzuki, M., Yoda K., Suzuki, H. 1996. Phenological comparison of the onset of vessel
997 formation between ring-porous and diffuse porous deciduous trees in a Japanese
998 temperate forest. *IAWA J* **17**: 431–44. <https://doi.org/10.1163/22941932-90000641>
- 999 Team R.C. 2018. R: a language and environment for statistical computing. Available from
1000 <https://www.r-project.org>.
- 1001 Thelin, G., Rosengren, U., Callesen, I., and Ingerslev, M. 2002. The nutrient status of Norway
1002 spruce in pure and in mixed-species stands. *For. Ecol. Manage.* **160**(1–3): 115–125.
1003 doi:10.1016/S0378-1127(01)00464-9.
- 1004 Thornthwaite, C.W. 1948. An approach toward a rational classification of climate. *Geogr.*
1005 *Rev.* **38**(1): 55–94. doi: 10.2307/210739.
- 1006 Thurm, E.A., Hernandez, L., Baltensweiler, A., Ayan, S., Rasztovits, E., Bielak, K., Zlatanov,
1007 T.M., Hladnik, D., Balic, B., Freudenschuss, A., Büchsenmeister, R., and Falk, W. 2018.
1008 Alternative tree species under climate warming in managed European forests. *For. Ecol.*
1009 *Manage.* **430**: 485–497. doi:10.1016/j.foreco.2018.08.028.

- 1010 Timofeeva, G., Treydte, K., Bugmann, H., Rigling, A., Schaub M., Siegwolf, R., and Saurer,
1011 M. 2017. Long-term effects of drought on tree-ring growth and carbon isotope variability
1012 in Scots pine in a dry environment. *Tree Physiol.* **37**(8): 1028–1041.
1013 doi:10.1093/treephys/tpx041.
- 1014 Toïgo, M., Perot, T., Courbaud, B., Castagneyrol, B., Gégout, J.C., Longuetaud, F., Jactel, H.,
1015 and Vallet, P. 2018. Difference in shade tolerance drives the mixture effect on oak
1016 productivity. *J. Ecol.* **106**(3): 1073–1082. doi:10.1111/1365-2745.12811.
- 1017 Trouvé, R., Bontemps, J.D., Collet, C., Seynave, I., and Lebourgeois, F. 2017. Radial growth
1018 resilience of sessile oak after drought is affected by site water status, stand density, and
1019 social status. *Trees* **31**: 517–529 doi:10.1007/s00468-016-1479-1.
- 1020 Vicente-Serrano, S.M., Beguería, S., and López-Moreno, J.I. 2010. A multiscalar drought
1021 index sensitive to global warming: The standardized precipitation evapotranspiration
1022 index. *J. Clim.* **23**(7): 1696–1718. doi:10.1175/2009JCLI2909.1.
- 1023 Vitasse, Y., Bottero, A., Cailleret, M., Bigler, C., Fonti, P., Gessler, A., Lévesque, M.,
1024 Rohner, B., Weber, P., Rigling, A., and Wohlgemuth, T. 2019. Contrasting resistance
1025 and resilience to extreme drought and late spring frost in five major European tree
1026 species. *Glob. Chang. Biol.* **25**(11): 3781–3792. doi:10.1111/gcb.14803.
- 1027 Vospernik, S. 2021. Basal area increment models accounting for climate and mixture for
1028 Austrian tree species. *For. Ecol. Manage.* **480**. 118725
1029 doi:10.1016/j.foreco.2020.118725.
- 1030 Vospernik, S. and Sterba, H. 2015. Do competition-density rule and self-thinning rule agree?
1031 *Ann. For. Sci.* **72**(3): 379–390. doi:10.1007/s13595-014-0433-x.
- 1032 Vospernik, S. and Nothdurft, A. 2018. Can trees at high elevations compensate for growth
1033 reductions at low elevations due to climate warming? *Can. J. For. Res.* **48**(6): 650–662.
1034 doi:10.1139/cjfr-2017-0326.
- 1035 Wigley, T.M.L., Briffa K.R., Jones P.D. 1984. On the average value of correlated time series.
1036 with applications in dendroclimatology and hydrometeorology. *J. Clim Appl Meteorol*
1037 **23**:201–213
- 1038 Wilmking, M., van der Maaten-Theunissen, M., van der Maaten, E., Scharnweber, T., Buras,
1039 A., Biermann, C., Gurskaya, M., Hallinger, M., Lange, J., Shetti, R., Smiljanic, M., and
1040 Trouillier, M. 2020. Global assessment of relationships between climate and tree growth.
1041 *Glob. Chang. Biol.* **26**(6): 3212–3220. doi:10.1111/gcb.15057.
- 1042 Wood, S.N. 2006. *Generalized Additive Models: An Introduction with r*. CRS Press.
- 1043 Wood, S.N. 2011. Fast stable restricted maximum likelihood and marginal likelihood
1044 estimation of semiparametric generalized linear models. *J. R. Stat. Soc.* **73**(1): 3–36. doi:
1045 10.1111/j.1467-9868.2010.00749.x.
- 1046 Wood, S.N. 2017. *Generalized Additive Models: An Introduction with R*.
- 1047 Yuste, J.C., Konôpka, B., Janssens, I.A., Coenen, K., Xiao, C.W., and Ceulemans, R. 2005.
1048 Contrasting net primary productivity and carbon distribution between neighboring stands
1049 of *Quercus robur* and *Pinus sylvestris*. *Tree Physiol.* **25**(6): 701–712.
1050 doi:10.1093/treephys/25.6.701.

1051 Zweifel, R., Rigling, A., and Dobbertin, M. 2009. Species-Specific Stomatal Response of
1052 Trees to Drought - a Link to Vegetation Dynamics? *J. Veg. Sci.* **20**(3): 442–54. doi:
1053 10.1111/j.1654-1103.2009.05701.x.

1054